The polyadenylase PAPI is required for virulence plasmid maintenance in pathogenic bacteria

Katherine Schubert[1], Micah Braly[2], Jessica Zhang[3], Michele E. Muscolo[4], Hanh N. Lam[2*], Karen Hug[2], Henry Moore[5], Joshua W. McCausland[3,6,7], Derfel Terciano[2], Todd Lowe[5], Cammie F. Lesser[4,8,9], Christine Jacobs-Wagner[3,6,7,10], Helen Wang[11], Victoria Auerbuch[2#]

[1]Department of Molecular, Cell, and Developmental Biology, UC Santa Cruz, Santa Cruz, CA 95064, United States

[2]Department of Microbiology and Environmental Toxicology, UC Santa Cruz, Santa Cruz, CA 95064, United States

[3]Department of Biology, Stanford University, Stanford, CA 94305, United States

[4]Center for Bacterial Pathogenesis, Division of Infectious Diseases, Department of Medicine, Massachusetts General Hospital, MA 02115, United States

[5]Department of Biomolecular Engineering, UC Santa Cruz, Santa Cruz, CA 95064, United States

[6]Sarafan ChEM-H Institute, Stanford University, Stanford, CA 94305, United States

[7]Howard Hughes Medical Institute, Stanford University, Stanford, CA 94305, USA

[8]Department of Microbiology, Blavatnik Institute, Harvard Medical School, Boston, MA 02115, United States

[9]Broad Institute of MIT and Harvard, Cambridge, MA 02142, United States

[10]Department of Microbiology and Immunology, Stanford University School of Medicine, Stanford, CA 94305, United States

[11]Department of Medical Biochemistry and Microbiology, Uppsala University, Sweden

* Current address: Department of Biological Sciences, Virginia Polytechnic Institute and State University, Blacksburg, VA 24061, United States

Abstract

Many species of pathogenic bacteria harbor critical plasmid-encoded virulence factors, and yet the regulation of plasmid replication is often poorly understood despite playing a critical role in plasmid-encoded gene expression. Human pathogenic *Yersinia*, including the plague agent *Y. pestis* and its close relative *Y. pseudotuberculosis*, require the type III secretion system (T3SS) virulence factor to subvert host defense mechanisms and colonize host tissues. The *Yersinia* T3SS is encoded on the IncFII plasmid for *Yersinia* virulence (pYV). Several layers of gene regulation enables a large increase in expression of *Yersinia* T3SS genes at mammalian body temperature. Surprisingly, T3SS expression is also controlled at the level of gene dosage. The number of pYV molecules relative to the number of chromosomes per cell, referred to as plasmid copy number, increases with temperature. The ability to increase and maintain elevated pYV plasmid copy number, and therefore T3SS gene dosage, at 37˚C is important for *Yersinia* virulence. In addition, pYV is highly stable in *Yersinia* at all temperatures, despite being dispensable for growth outside the host. Yet how *Yersinia* reinforces elevated plasmid replication and plasmid stability remains unclear. In this study, we show that the chromosomal gene *pcnB* encoding the polyadenylase PAP I is required for regulation of pYV plasmid copy number (PCN), maintenance of pYV in the bacterial population outside the host, robust T3SS activity, and *Yersinia* virulence in a mouse infection model. Likewise, *pcnB*/PAP I is also required for robust expression of the *Shigella flexneri* virulence plasmid-encoded T3SS. Furthermore, *Yersinia* and *Shigella pcnB*/PAP I is required for maintaining normal PCN of model antimicrobial resistance (AMR) plasmids whose replication is regulated by sRNA, thereby increasing antibiotic resistance by ten-fold. These data suggest that *pcnB*/PAP I contributes to the spread and stabilization of virulence and AMR plasmids in bacterial pathogens, and is essential in maintaining the gene dosage required to mediate plasmid-encoded traits. Importantly *pcnB*/PAP I has been bioinformatically identified in many species of bacteria despite

being studied in only a few species to date. Our work highlights the potential importance of *pcnB*/PAP I in antibiotic resistance, and shows for the first time that *pcnB*/PAP I reinforces PCN and virulence plasmid stability in natural pathogenic hosts with a direct impact on bacterial virulence.

Author Summary

Many pathogens carry extrachromosomal DNA elements known as plasmids, which encode genes that confer bacterial virulence or antimicrobial resistance (AMR). Acquisition of these plasmids by bacteria can lead to the emergence of new pathogenic traits and the spread of AMR, yet the mechanisms by which plasmids are retained in bacterial populations particularly in the absence of selective pressure remain incompletely understood. Here we show that the major bacterial polyadenylase enzyme PAP I, encoded by the *pcnB* gene, is critical for the human pathogen *Yersinia pseudotuberculosis* to maintain its native virulence plasmid as well as AMR plasmids. Very little is known about the process of polyadenylation in bacteria, or the post-transcriptional addition of adenosine residues to the 3' end of transcripts. This study represents the first demonstration that PAP I-mediated polyadenylation contributes to bacterial pathogenesis.

Introduction

Many species of pathogenic bacteria harbor plasmids that encode genes important for virulence or antimicrobial resistance (AMR). Virulence plasmids are typically characterized by their relatively large size (>40kb) and low plasmid copy number (PCN), which refers to the average

number of plasmid copies per cell or chromosome equivalent [1]. In addition to virulence or AMR genes, these plasmids typically contain additional genes important for plasmid replication, PCN control, and plasmid maintenance. Virulence plasmids are commonly found in members of the Enterobacteriaceae family, which includes several species of Gram-negative pathogens. For example, *Yersinia pseudotuberculosis* and the related plague agent *Yersinia pestis* naturally harbor a ~70 kb low copy number virulence plasmid known as the *plasmid for Yersinia virulence* (pYV), also called pCD1 in *Y. pestis* [2-4]. Given that *Y. pestis* has killed over 200 million people since antiquity [5], pYV has played a grim but important role in human history.

The pYV plasmid encodes several factors important for *Yersinia* virulence, including a major virulence factor known as the type III secretion system (T3SS) [6-8]. The T3SS is used to inject a series of effector proteins known as *Yersinia* outer proteins (Yops) directly into the cytosol of target host cells during infection. Yops dampen the host immune response and promote *Yersinia* pathogenesis, making pYV essential for *Yersinia* virulence [3, 9-13]. Expression and activity of the T3SS exerts a metabolic burden on the bacteria. Therefore, *Yersinia* repress expression of the T3SS at low environmental temperatures when the T3SS is dispensable, but induce T3SS expression at mammalian body temperature, 37°C [14-19]. Several mechanisms contribute to this temperature dependency. For example, the master regulator of the T3SS is only translated at 37°C due to control by an RNA thermometer [18, 20]. More recently, it was reported that temperature-dependent changes in T3SS gene expression is also regulated at the level of gene dosage via changes in pYV PCN [21]. At environmental temperatures such as 26°C, pYV PCN has been reported to be low (~1-2 copies per chromosome). Upon exposure to mammalian temperatures of 37°C, pYV PCN has been shown to be rapidly upregulated to 3+ copies per chromosome. Importantly, this ability to upregulate pYV PCN and T3SS gene dosage is essential for normal T3SS activity and *Y. pseudotuberculosis* virulence [21, 22].

74 Dynamic changes in pYV PCN and retention of the pYV plasmid during these rapid changes are
75 therefore required for the *Y. pseudotuberculosis* pathogenic lifestyle.

76

77 The pYV plasmid encodes several systems important for plasmid regulation and maintenance,
78 including a *cop-rep* locus that regulates plasmid replication, a ParAB partitioning system that
79 ensures each daughter cell inherits the plasmid, and a ParDE toxin-antitoxin (TA) system that
80 promotes plasmid maintenance in the bacterial population [1, 23]. Together, these systems are
81 predicted to synergistically enforce plasmid stability, or the percentage of cells in the population
82 that maintain the plasmid. The highly conserved *cop-rep* locus places pYV in the IncFII group of
83 plasmids [1, 24, 25]. The *cop-rep* locus encodes the essential *rep*lication initiation factor RepA
84 and two negative regulators of RepA expression: the CopA small RNA (sRNA) and the CopB
85 protein. The functions of RepA, CopA, and CopB have been elucidated using plasmid R1, an
86 IncFII plasmid originally isolated from a clinical strain of *S. enterica* that has been extensively
87 studied in *Escherichia coli* model systems [25-27]. These studies support the notion that CopA
88 and CopB regulate the rate of plasmid replication to minimize fluctuations above or below the
89 average PCN set-point [25, 28].

90

91 Using *Y. pseudotuberculosis* as a model, we identified the chromosomal *pcnB* gene as a
92 previously unknown regulator of pYV replication and stability. The *pcnB* gene was named for
93 plasmid copy number B since loss of *pcnB* was found to decrease PCN for several model
94 plasmids in *E. coli* [29, 30]. The *pcnB* gene encodes the poly A polymerase (PAP I), the major
95 bacterial polyadenylase ubiquitous in β- and γ-proteobacteria [29-36]. Polyadenylation, or the
96 addition of adenosine residues to the 3' OH of an RNA transcript, is poorly understood in
97 bacteria compared to eukaryotes. PAP I-mediated polyadenylation promotes RNA degradation

98 as part of a housekeeping mechanism [37], but is also implicated in certain gene regulatory
99 networks [38-43]. PAP I-dependent polyadenylation has been shown to destabilize RNAs that
100 negatively regulate replication of certain plasmid types in *E. coli*, including CopA from plasmid
101 R1 and RNAI from ColE1 plasmids [29, 44-47]. However, PAP I has not been studied in the
102 context of a naturally occurring virulence or AMR plasmid within its native host, and has never
103 been linked to bacterial virulence.

104

105 Here, we report that *Y. pseudotuberculosis pcnB* mutants display reduced PCN and decreased
106 stability of pYV. This defect is associated with reduced T3SS activity in bacterial culture and
107 impaired virulence in a mouse infection model. Furthermore, we show that *pcnB* is required for
108 *Y. pseudotuberculosis* to maintain model AMR plasmids belonging to various plasmid families,
109 highlighting its crucial role in bacterial pathogenicity and antibiotic resistance.

110

111 Results

112 *Y. pseudotuberculosis* toggles pYV plasmid copy number in response to temperature

113 To determine the average PCN per chromosome equivalents at the bacterial population level,
114 we used droplet digital (dd)PCR to measure the number of pYV molecules relative to
115 chromosomes in wildtype *Y. pseudotuberculosis* IP2666pIB1 [22]. Cells were either grown at
116 26°C to represent growth in environmental conditions outside of the host or at 37°C in low
117 calcium media to represent host cell contact during mammalian infection. The pYV-encoded
118 T3SS is expressed at 37°C and becomes active for secretion following host cell membrane
119 contact or calcium chelation [48-51]. Consistent with previous studies [21, 22], we observed an
120 increase in pYV PCN from an average of ~1.5 pYV copies per chromosome equivalents at 26°C
121 to ~3 copies at 37°C/low calcium (Fig 1A). In addition, using a YPIII/pIBX strain of *Y.*

122 *pseudotuberculosis* harboring a pYV-encoded luciferase reporter, we found that pYV PCN
123 relative to cell density increases one hour after shifting the cultures to 37°C/low calcium
124 conditions (Fig 1B).

125

126 To examine pYV PCN at the single-cell level, we employed a microscopy-based approach. To
127 visualize and quantify pYV puncta in living *Y. pseudotuberculosis* cells, we generated a
128 YPIII/pIBX *Y. pseudotuberculosis* strain that harbors a *parB-msfGFP* translational fusion in the
129 native *parB* pYV locus. This approach has been used to visualize plasmids in other bacterial
130 species [52, 53], as ParB binds to plasmid-encoded *parS* sequences but has never been used
131 to study pYV in *Y. pseudotuberculosis*. At 26°C, cells were found to have an average of about
132 four pYV puncta per cell (Fig 1C-D). This number increased to an average of about seven
133 puncta per cell by 1.5 hours after the shift to 37°C (Fig 1C-D). The higher number of pYV per
134 cell than per chromosome equivalents (Figs 1D vs. 1A) is consistent with the expectation that
135 *Yersinia* has more than one chromosome per cell on average under nutrient-rich (fast) growth
136 conditions, similar to *E. coli* [54, 55]. Regardless of the normalization method (per cell or
137 chromosome), *Yersinia* pYV PCN consistently increased by ~1.5-fold upon shifting bacterial
138 cultures from 26°C to 37°C/low calcium conditions. The pYV plasmid was highly stable in *Y.*
139 *pseudotuberculosis*, with the vast majority of cells or clones retaining pYV (Fig 1D).

140

141 **Disruption of the *pcnB* gene encoding the polyadenylase PAP I decreases pYV PCN and**
142 **T3SS expression**

143 *Y. pseudotuberculosis* with a functional T3SS, but lacking T3SS Yop effectors (Δyop6), induces
144 activation of the transcription factor NFκB in mammalian cells [56]. The LPS metabolite ADP
145 heptose is delivered to the host cell cytoplasm through the T3SS, stimulating Alpk1/TIFA-

146 dependent NFκB activation [57], although YopJ inhibits NFκB signaling [58, 59]. We used
147 human embryonic fibroblast cells, HEK293T, expressing an NFκB luciferase reporter to identify
148 a *Y. pseudotuberculosis* IP2666pIB1 ∆yop6 transposon (Tn) mutant that induced elevated
149 bioluminescence compared to the parental strain, (∆yop6/*pil*::Tn; Fig S1A) [56]. This mutant was
150 found to harbor a Tn insertion in a previously unannotated locus adjacent to the highly
151 conserved pYV *cop-rep* locus. We will refer to this locus as the plasmid inhibitory locus (*pil*) (Fig
152 S1B). Given the location of the *pil* locus relative to *cop-rep*, we hypothesized that the *pil*::Tn
153 mutation affects the pYV PCN. To test this, we introduced the *pil::Tn* insertion mutation into a
154 clean wildtype *Y. pseudotuberculosis* IP2666pIB1 strain background with intact T3SS effector
155 Yop-encoding genes (referred to as *pil*::Tn). Consistent with our hypothesis, the *pil::Tn* mutant
156 displayed elevated secretion of the T3SS cargo proteins YopE, YopD, and YopH compared to
157 wildtype *Yersinia* (Fig S1C). In addition, we constructed a mutant in the YPIII/pIBX background
158 with a plasmid insertion into the same locus in *pil* (*pil*::pNQ). As expected, both the *pil*::Tn and
159 *pil*::pNQ strains had elevated pYV PCN at 26°C and early after shifting to 37°C relative to the
160 parental strain (Fig S1DE), which is likely the underlying cause of the increased T3SS activity .

161

162 Insertion into the *pil* locus was associated with poor growth compared to the parental strain
163 under T3SS-inducing conditions, and suppressor mutants could be readily isolated (Fig S1F).
164 We hypothesized that constitutively elevated pYV PCN contributed to this growth defect,
165 resulting in selective pressure favoring suppressor mutations that would alleviate high pYV
166 PCN. Therefore, we used the *pil* insertion mutation as a tool to identify genes important for pYV
167 PCN homeostasis. We carried out whole genome sequencing of a subset of *pil*::pNQ
168 suppressor mutants and identified several categories of mutations affecting growth, pYV PCN,
169 and the T3SS (Table S1). Two clones harbored a single point mutation that was associated with
170 reduced pYV PCN and T3SS activity relative to the *pil*::pNQ parental strain. This mutation was

171 mapped to the *pcnB* gene encoding the polyadenylase PAP I, and was predicted to confer a
172 leucine to arginine change at position 291 (L291R) in the PAP I neck domain linked to RNA
173 binding (Fig 2A). The L291 residue is conserved in PAP I from *E. coli*, suggesting that the
174 residue might be important for PAP I structure and/or function (Fig 2A). We will use the term
175 *pcnB* when referring to the gene, and PAP I when referring to the *pcnB*-encoded protein.

176

177 To confirm that the *pcnB* gene encoding PAP I affects *Y. pseudotuberculosis* pYV PCN, we
178 generated a full in-frame deletion of the *pcnB* gene (Δ*pcnB*) in the wildtype and *pil*::Tn
179 IP2666pIB1 strain backgrounds. We used ddPCR to measure relative pYV PCN and found that
180 compared to wildtype, the Δ*pcnB* mutant had lower pYV PCN following growth at 26°C and
181 37°C/low calcium (Fig 2B). In keeping with our previous findings, the *pil*::Tn mutant displayed
182 significantly higher pYV PCN at 26°C compared to wildtype. Furthermore, loss of PAP I in the
183 *pil*::Tn/Δ*pcnB* double mutant significantly reduced pYV PCN at 26°C compared to the *pil*::Tn
184 parental strain. These results show that loss of PAP I leads to decreased pYV PCN. Despite
185 this, loss of *pcnB* did not prevent *Yersinia* from increasing pYV PCN upon shift from 26°C to
186 37°C, although not to the same high PCN as in wildtype (Fig 2B). Consistent with this reduction
187 in T3SS gene dosage, the Δ*pcnB* mutant displayed two-fold less expression and secretion of
188 the T3SS effector protein YopE compared to wildtype *Y. pseudotuberculosis* (Fig 2C). Similarly,
189 *pcnB* deletion reduced YopE expression and secretion in the *pil*::Tn strain background (Fig 2C).
190 Taken together, these data suggest that *pcnB* is essential for maintaining pYV PCN, and that
191 this function is important for enabling robust T3SS expression under T3SS-inducing conditions.

192

193 To determine how the *pcnB* gene and the *pil*::Tn disruption broadly impact expression of pYV-
194 encoded genes, we carried out RNA-seq analyses on wildtype, Δ*pcnB*, *pil*::Tn, and
195 *pil*::Tn/Δ*pcnB Y. pseudotuberculosis* IP2666pIB1 grown at 26°C and 37°C/low calcium

196 (Supplementary Dataset 1). Most pYV-encoded gene transcripts were present at higher steady-
197 state level in the *pil*::Tn mutant compared to wildtype *Y. pseudotuberculosis* at both
198 temperatures (Fig S2), consistent with an increase in pYV gene dosage. However, T3SS genes
199 are not translated at 26°C due to the action of several RNA thermometers in *Yersinia* [48], and
200 the *pil*::Tn strain does not display T3SS activity at 26˚C despite elevated T3SS gene transcripts
201 at this temperature (Fig S3). Interestingly, the *pil*::Tn strain displayed altered the RNA-Seq read
202 pattern of the region containing *pil*, *copB*, and *repA* at both temperatures (Fig S4). We observed
203 no difference in pYV PCN or T3SS expression when we generated a full in-frame deletion of the
204 predicted ORF found in the *pil* locus (Fig S1C,E). Therefore, we propose that Tn or pNQ
205 insertion into *pil* leads to derepressed transcription of the *cop-rep* locus leading to elevated pYV
206 replication through an as-yet unknown mechanism. In contrast, deletion of *pcnB* resulted in
207 fewer transcripts of most pYV-encoded genes compared to wildtype *Yersinia* at both
208 temperatures (Fig S2), consistent with a decrease in pYV gene dosage. In addition, *pcnB*
209 deletion in the *pil*::Tn background also led to a decrease in the steady-state levels of most T3SS
210 genes compared to the *pil*::Tn parental strain (Fig S2). We conclude that loss of *pcnB* leads to a
211 decrease in pYV PCN in both the wildtype and *pil*::Tn backgrounds, leading to decreased
212 transcription of pYV-encoded genes and mitigation of the T3SS activity-induced growth arrest.

213

214 **PAP I is required for pYV stability**

215 When working with the Δ*pcnB* strain, we noted that cells lost the pYV plasmid at a higher rate
216 than observed with wildtype *Y. pseudotuberculosis* (Table 1). To determine whether PAP I
217 affects pYV stability in addition to pYV PCN, we generated a Δ*pcnB* strain in the ParB-msfGFP
218 YPIII/pIBX *Y. pseudotuberculosis* background and observed cells lacking clear fluorescent foci
219 under both non-T3SS-inducing (26˚C) and T3SS-inducing conditions (37˚C, low calcium media.
220 We observed Δ*pcnB* cells with lower cellular GFP fluorescence, consistent with plasmid loss

221 given that the msfGFP-labeled ParB is encoded by pYV (Fig 3A). The presence of these
222 plasmid-devoid cells in the Δ*pcnB* strain resulted in a clear bimodal distribution of cellular
223 fluorescence (Fig 3B), showing that ~34% of Δ*pcnB* cells lacked pYV (low cellular fluorescence)
224 compared to only ~3% for the wild-type population at the time of imaging at 26ºC ($p<10^{-100}$,
225 Kolmogorov-Smirnov (KS) test; n = 7033 cells per strain). The Δ*pcnB* mutant also displayed a
226 high percentage (24%) of cells lacking pYV under the 37°C/low calcium condition based on the
227 fraction of cell population with low cellular fluorescence (Fig 3B). By analyzing only those cells
228 that retained at least one copy of pYV, we found that the Δ*pcnB* mutant showed the expected
229 increase in ParB-msfGFP puncta per cell from 26°C to 37°C/low calcium (Fig 3B-C). However,
230 the distributions were significantly shifted toward lower values relative to the wildtype strain
231 ($p<10^{-100}$; Fig 3D-E). While the wildtype strain had, on average, 4.5 and 7.9 pYV spots per cell
232 at 26˚C and 37˚C/low calcium, respectively, the Δ*pcnB* strain had 3.9 and 6.3. Thus, the *pcnB*
233 gene does not affect the ability of the cells to respond to the T3SS-inducing environmental shift,
234 but its loss leads to lower average PCN and increased frequency of plasmidless *Yersinia* cells.

235

236 To further examine the extent of the pYV plasmid stability defect in the Δ*pcnB* mutant, we
237 passaged bacteria on solid media for several days at 26°C and then assessed pYV retention for
238 each clone by patching onto low calcium media containing the dye Congo red, and incubating at
239 37˚C. Congo red only binds to bacteria that are expressing a functional T3SS [60]. Wildtype
240 cells retained the pYV plasmid at 100% while the Δ*pcnB* mutant cells only retained pYV in 82%
241 of cells following incubation at 26˚C for 16 hours during passaging (Table 1). When cells were
242 exposed to T3SS-inducing conditions at 37°C/low calcium and returned to 26°C to mimic the *Y.*
243 *pseudotuberculosis* facultative lifecycle, we found that only 58% of Δ*pcnB* cells retained pYV
244 compared to 99% for wildtype (Table 1). This observed increase in pYV loss likely stems from
245 the growth arrest of pYV^+ clones specifically under T3SS-inducing conditions at 37˚C [15, 49,

246 50], which provides a selective growth advantage for Δ*pcnB* clones that have lost pYV.

247 Altogether, these data support a role for PAP I in regulation of pYV PCN and plasmid stability

248 during the *Y. pseudotuberculosis* facultative lifecycle.

249

250 **Table 1. PAP I is required for pYV maintenance in *Y. pseudotuberculosis***

Strain:	Percent Retention[ǂ] of pYV after growth at 26°C only:	Percent Retention[ǂ] of pYV after 16 hr exposure to 37°C:
Wildtype	100.0 ±0	99.1 ±1.2
Δ*pcnB*	81.6 ±17.3	57.7 ±10.7
pil::Tn	100.0 ±0	99.1 ±1.3
pil::Tn Δ*pcnB*	98.1 ±1.8	75.9 ±13.1

251
252 [ǂ]Percent retention of the pYV plasmid was averaged from three independent experiments where ±
253 represents the standard deviation between experiments.

254

255 **The PAP I^{L291R} mutation affects PAP I protein levels.**

256 The original *pcnB* suppressor mutation identified in our *pil*::Tn suppressor screen was a single

257 point mutation that changed leucine in position 291 to an arginine (L291R) (Fig 2A). Although

258 the corresponding L291 residue is conserved in *E. coli*, it has not yet been identified as a critical

259 PAP I residue. Thus, as a first step in investigating the role of this residue, we assessed

260 whether the L291R mutation affects PAP I expression. We introduced the L291R missense

261 mutation into the native *pcnB* locus of both *Y. pseudotuberculosis* IP2666pIB1 (with or without a

262 PAP I C-terminal FLAG tag) and YPIII/pIBX to generate PAP I^{L291R} strains. We found that the

263 PAP I^{L291R} protein was poorly expressed, particularly at 37°C/low calcium (Fig. 4A). These data

264 suggest that the PAP I^{L291R} allele may be unstable, leading to low PAP I expression at least at

265 37°C/low calcium. Interestingly, a strain engineered with a more conservative leucine to alanine
266 mutation at position 291, PAP I^{L291A}, did not significantly affect PAP I expression levels (Fig 4A).
267 Consistent with these data, the PAP I^{L291R} mutant showed enhanced loss of pYV compared to
268 the wildtype strain or the PAP I^{L291A} mutant, as indicated by the emergence of white, fast-
269 growing colonies following growth under 37°C/low calcium conditions on Congo red agar (Fig
270 4B). Interestingly, the PAP I^{L291R} strain displayed a greater loss of pYV following long passage at
271 37°C/low calcium compared to when bacteria were passaged at 26°C (Table 2), reflective of the
272 relative stability of the PAP I^{L291R} protein at 26˚C. Lastly, the PAP I^{L291R} strain had significantly
273 lower average pYV PCN compared to the wildtype and PAP I^{L291A} strains at 37˚C/low calcium
274 (Fig 4C), and this correlated with lower relative T3SS activity (Fig 4D). Taken together, these
275 data suggest that the PAP I^{L291R} mutation disrupts PAP I protein levels, explaining why we
276 identified this mutation in our suppressor screen.

277

278 **Mutation of residues predicted to affect polyadenylase activity decreases pYV PCN,**
279 **plasmid maintenance, and T3SS activity**

280 PAP I D80 and D82 have been shown to be essential for PAP I polyadenylase catalytic activity
281 in *E. coli* [61, 62]. These residues are also present in *Y. pseudotuberculosis* PAP I (Fig. 2A). To
282 determine whether the PAP I polyadenylase activity is responsible for PAP I's roles in pYV PCN
283 and maintenance, we mutated the two corresponding aspartic acid residues (D114 and D116) to
284 alanine to produce a PAP I^{D2A} catalytic mutant. These mutations did not affect PAP I steady
285 state protein levels (Fig 4A). However, we found that the PAP I^{D2A} mutant displayed reduced
286 pYV PCN at 26°C and 37°C/low calcium compared to wildtype *Y. pseudotuberculosis*, to the
287 same degree as observed in the Δ*pcnB* strain which lacks PAP I completely (Fig 4C). Spot test
288 serial dilution analyses found that PAP I^{D2A} grows similarly to wildtype and Δ*pcnB* at 26°C (Fig
289 4B). Furthermore, at 37°C/low calcium, PAP I^{D2A} and Δ*pcnB* exhibited about 10-fold more

290 growth compared to wildtype (Fig 4B), consistent with a reduction in growth arrest due to
291 decreased T3SS activity. Similarly, the strain expressing PAP I^{D2A}, like the Δ*pcnB* mutant,
292 displayed an increased number of plasmidless, rapidly-growing colonies (Fig. 4B) and reduced
293 pYV stability (Table 2). Lastly, the PAP I^{D2A} allele did not support normal T3SS activity (Fig 4D).
294 Taken together, these data suggest that *Yersinia* PAP I functions as a polyadenylase that
295 maintains pYV PCN, plasmid stability, and T3SS gene expression and activity.

296

297 **Table 2. Important PAP I residues are required for stability of the pYV plasmid**

Strain:	Percent Retention[ǂ] of pYV after growth at 26°C only:	Percent Retention[ǂ] of pYV after exposure to 37°C:
Wildtype	100.0 ±0	97.3 ±3.8
Δ*pcnB*	80.2 ±7.8	47.7 ±14.0
$PAPI^{D2A}$	94.0 ±1.7	21.0 ±7.0
$PAPI^{L291R}$	98.6 ±2.5	68.6 ±7.9
$PAPI^{L291A}$	100.0 ±0	100 ±0

298
299 [ǂ]Percent retention of the pYV plasmid was averaged from three independent experiments where ±
300 represents the standard deviation between experiments.

301

302 ***Yersinia* PAP I is required for plasmid stability and plasmid-mediated antibiotic**
303 **resistance from a broad range of plasmid families**

304 To determine if *Yersinia* PAP I contributes to regulation of PCN and retention of other plasmid
305 types, we introduced a ColE1-like pGFP-uv plasmid into wildtype and Δ*pcnB Y.*
306 *pseudotuberculosis*. This plasmid lacks active partitioning systems such as ParABS, but can be
307 maintained within the population by antibiotic resistance selection [63]. We observed a decrease
308 in fluorescence intensity in Δ*pcnB* colonies compared to wildtype when grown on carbenicillin-

309 containing media, suggesting that lowering of pGFP-uv PCN in the absence of PAP I in *Y.*
310 *pseudotuberculosis* leads to less robust antibiotic resistance (Fig. 5A). To determine if the
311 decreased PCN of the pGFP-uv plasmid in the Δ*pcnB* strain leads to plasmid loss, we
312 measured kinetics of plasmid retention over 40 hours after removing antibiotic selection. We
313 found that over 70% of Δ*pcnB* cells lose the pGFP-uv plasmid within 10 hours of removing
314 carbenicillin and the plasmid is completely lost from the population by ~36 hours. In contrast,
315 100% of wildtype cells retained pGFP-uv over the same 36 hour time course (Fig. 5B).

316

317 To ensure that the growth defect seen for Δ*pcnB* harboring pGFP-uv was due to loss of PAP I
318 specifically, we next constructed a PAP I over-expression plasmid in the pTrc99 vector
319 backbone. Importantly, pTrc99 is also a ColE1-like plasmid that lacks partitioning systems [64].
320 We found that Δ*pcnB* harboring pTrc99::empty displays a 10-fold growth defect when spotted
321 onto LB-carbenicillin but not LB-only plates (Fig. 5C), consistent with what was previously
322 observed with the pGFP-uv plasmid. Importantly, this growth defect was nearly completely
323 abolished by expression of PAP I from the pTrc99 plasmid (Fig. 5C). In addition to ColE1
324 plasmids, we found that PAP I is also required for robust antibiotic resistance conferred by
325 plasmids with p15A-like origins of replication (pACYC184, pBAD33) (Fig S5). Interestingly,
326 replication of plasmids containing ColE-like and p15A-like origins of replication, as well as IncFII
327 plasmids like pYV, is regulated by plasmid-specific sRNA [65-67], suggesting a general role for
328 PAP I in regulating plasmids with replicons regulated by a sRNA. To test if loss of *pcnB* would
329 affect antibiotic resistance conferred by a plasmid whose replication is <u>not</u> known to be
330 regulated by a sRNA, we introduced the mini-F plasmid pNF06::*ccdAB* into wildtype and Δ*pcnB*
331 *Y. pseudotuberculosis* [30, 44, 68, 69]. The Δ*pcnB* strain grew equally well to the wildtype strain
332 in the presence of antibiotic selection, suggesting that pNF06::*ccdAB* maintenance and copy
333 number is likely not affected by PAP I (Fig. 5D). These data suggest that PAP I is important for

334 *Yersinia* to maintain normal PCN and stability of plasmids whose replication is regulated by a
335 sRNA.

336

337 **PAP I is required for *Y. pseudotuberculosis* virulence in mice**

338 It is well established that the pYV plasmid and T3SS are critical for *Y. pseudotuberculosis*
339 virulence in mouse infection models [6, 70]. To determine if loss of PAP I contributes to *Yersinia*
340 virulence, we infected mice via the intraperitoneal (IP) route and monitored colonization of the
341 spleen and liver. Four days post-inoculation, significantly fewer Δ*pcnB*-infected mice exhibited
342 robust colonization of the spleen and liver compared to wildtype-infected mice (Fig 6A and B).
343 Interestingly, Δ*pcnB*-infected mice formed two distinct populations: one population where the
344 spleen and liver were colonized to the same levels as wildtype-infected mice, and a second
345 population that had completely cleared the infection (Fig. 6A and B). We isolated several Δ*pcnB*
346 clones from the livers of colonized mice and found that their pYV stability and T3SS activity
347 phenotypes were similar to the inoculum strain (Fig S6). In addition, we sequenced the
348 genomes of these isolates and could not identify any significant mutations, suggesting that host
349 tissue colonization by the Δ*pcnB* mutant in a subset of mice does not stem from suppressor
350 mutations that stabilize pYV. Taken together, these data suggest that PAP I increases the
351 likelihood of *Yersinia* colonization of host tissues.

352

353 **PAP I is required for maintenance of plasmid-encoded T3SS expression and antibiotic**
354 **resistance in *Shigella flexneri***

355 The human pathogen *Shigella flexneri* harbors a virulence plasmid, pINV, with a RepFIIA origin
356 similar to the one found on *Yersinia* pYV [1]. To test whether PAP I also regulates *Shigella*
357 pINV, we deleted the *pcnB* gene in the *S. flexneri* M90T Δ*ipaH2.5* (Δ*ipaH2.5::tet*^{R}) strain. The

358 resulting Δ*ipaH2.5*Δ*pcnB* mutant was defective in Congo red binding compared to its parental
359 strain (Fig 7A), suggesting a T3SS defect. Indeed, the Δ*ipaH2.5*Δ*pcnB* strain exhibited a stark
360 defect in expression and secretion of the T3SS translocon proteins IpaB, IpaC, and IpaD
361 compared to the parental strain (Fig 7BC). Lastly, we introduced pTRC99 that confers IPTG-
362 inducible expression of *Yersinia* PAP I into the Δ*ipaH2.5* and Δ*ipaH2.5*Δ*pcnB* strains. Consistent
363 with our previous data using *Y. pseudotuberculosis* strains (Fig 5C), deletion of *pcnB* led to a
364 >10-fold loss of antibiotic resistance that could be complemented by PAP I expression (Fig 7D).
365 Taken together, these data suggest that PAP I is essential for maintaining robust plasmid
366 replication, resulting in increased expression of plasmid-encoded virulence and antibiotic
367 resistance genes in pathogenic bacteria.

368

369 **Discussion**

370 *Y. pseudotuberculosis* modulates the PCN of its pYV virulence plasmid to control the dosage of
371 pYV-encoded genes in response to temperature [21, 22]. This ability of *Y. pseudotuberculosis* to
372 upregulate pYV PCN at mammalian body temperature is critical for its ability to cause disease.
373 Here, we show that in addition to dynamic regulation of pYV PCN, *Y. pseudotuberculosis*
374 requires the chromosomal gene *pcnB*, encoding the PAP I polyadenylase, to maintain pYV PCN
375 homeostasis and prevent pYV loss from the bacterial population. The role of the *pcnB* gene in
376 promoting virulence plasmid-encoded T3SS expression is conserved in both *Y.*
377 *pseudotuberculosis* and *S. flexneri*. Although *pcnB*/PAP I has been shown to regulate plasmid
378 replication of model plasmids in *E. coli*, this is the first study to link this gene to bacterial
379 pathogenesis. In addition, the requirement of *Yersinia* and *Shigella pcnB*/PAP I for robust
380 plasmid-encoded antibiotic resistance suggests that PAP I represents a potential new drug
381 target.

382

383 Putative PAP I orthologs have been bioinformatically identified in many bacterial species hailing
384 from diverse phyla, and yet studies on *pcnB*/PAP I have historically been confined to a small
385 number of non-pathogenic bacterial species [36]. *E. coli* PAP I (EcPAP) has been shown to
386 promote RNA degradation of target transcripts. Degradation of RNA is generally initiated by the
387 endonuclease RNase E and, in the absence of 3' secondary structures, the RNA fragments
388 produced by RNase E are then digested by the 3'-5' exonulceases PNPase and RNase II [71].
389 However, RNase II- and PNPase-mediated RNA degradation is significantly impaired for
390 transcripts that have terminal stem-loop structures, such as mRNAs containing intrinsic
391 terminators at their 3' ends and structured sRNAs [71]. PAP I has been shown to add poly(A)
392 tails to the 3' ends of transcripts containing terminal stem-loops structures to promote their
393 decay [72-74] and it is thought that PAP I-dependent polyadenylation of these transcripts
394 provides a "toe-hold" for PNPase and RNase II to bind and digest the RNA [74-77]. Components
395 of the RNA degradosome such as PNPase are known to be important for T3SS function in *Y.*
396 *pseudotuberculosis* [78-80] and PAP I has been shown to copurify with PNPase in *E. coli* [81],
397 suggesting that PAP I may represent a novel component of the *Yersinia* RNA degradosome.
398 Importantly, many of the major domains and catalytic residues are conserved between *Yersinia*
399 and *Shigella* PAP I and EcPAP. EcPAP polyadenylase activity is abolished when the two
400 catalytic residues Asp80 and Asp82 are mutated to alanine residues in *E. coli* [61, 62]. To test if
401 the phenotypes of the Δ*pcnB* strain was due to loss of PAP I polyadenylase activity, we mutated
402 the corresponding catalytic residues (Asp114 and Asp116) in PAP I from *Y. pseudotuberculosis*
403 to generate a $PAPI^{D2A}$ strain with both catalytic residues replaced by alanine residues. The
404 $PAPI^{D2A}$ mutant recapitulated the phenotypes observed for the Δ*pcnB* strain, including reduced
405 pYV PCN, plasmid stability, and T3SS activity. This supports that PAP I acts as a polyadenylase

406 to regulate plasmid maintenance and T3SS activity in *Y. pseudotuberculosis*, and our data
407 suggests that this may also be the case in *S. flexneri.*

408

409 EcPAP has been shown to polyadenylate both chromosomally- and plasmid-derived transcripts
410 and was first identified due to its regulation of a sRNA that regulates plasmid replication [29, 30].
411 EcPAP has been shown to regulate PCN for the IncFII family plasmid R1 by polyadenylating
412 and targeting CopA regulatory sRNA for degradation, leading to de-repression of R1 plasmid
413 replication and increasing R1 PCN (46). This is consistent with our finding that PAP I is required
414 for normal PCN and maintenance of the IncFII family *Yersinia* pYV plasmid, and for normal
415 expression of the *Shigella* T3SS encoded on the related pINV virulence plasmid [1]. Taken
416 together, these data point to the possibility that PAP I targets CopA sRNA from the *Yersinia* pYV
417 and *Shigella* pINV *cop-rep* loci for polyadenylation. Bacteria are thought to maintain large
418 extrachromosomal elements such as IncF virulence plasmids within a tight PCN range near a
419 specific "set point" that is optimal for that species lifestyle [25]. This is particularly complicated in
420 the case of pYV since this plasmid seems to have a different optimal PCN "set point" depending
421 on temperature. Given that the Δ*pcnB* mutant displays a PCN defect at both 26°C and 37°C,
422 this suggests that pYV plasmid replication rates are unusually low in the absence of PAP I in
423 general, possibly due to the buildup of CopA sRNA. Reduced plasmid replication rates can also
424 lead to plasmid stability defects when the plasmid replication rate drops low enough that cells
425 can no longer reliably pass a copy of the plasmid to daughter cells during cell division [82]. Both
426 reduced PCN and reduced plasmid stability can theoretically drive compounding disturbances in
427 plasmid maintenance systems due to reduced gene dosage of stability systems such as
428 partitioning and toxin-antitoxin (TA) systems. In keeping with this idea, our RNA-seq analysis
429 supports the notion that the decrease in pYV-encoded gene dosage in the absence of PAP I
430 leads to decreased expression of the ParDE TA system in Δ*pcnB* cells that may be responsible

431 for killing plasmidless cells (Supplementary Dataset 1)[23]. Altogether, this supports the claim
432 that PAP I is required for maintenance of the pYV PCN "set point" at both 26°C and 37°C,
433 possibly through modulation of CopA sRNA levels. This, in turn, may decrease the frequency at
434 which plasmidless daughter cell arise. Alternatively, PAP I may also regulate stability of
435 additional transcripts that control plasmid partitioning and/or post-segregational killing. Future
436 studies will focus on identification of polyadenylated transcripts in *Yersinia* and *Shigella*.

437

438 While there is an overall reduction in pYV PCN in the absence of *pcnB*/PAP I, Δ*pcnB* cells that
439 retain the pYV plasmid still increase pYV PCN upon shifting from 26°C to 37°C. In addition, we
440 have found that the *pcnB* gene is transcribed at 26°C and 37°C (Supplementary Dataset 1) and
441 the PAP I protein is also produced at both temperatures (Fig 4A). Taken together, this suggests
442 that PAP I is not required for the temperature-dependent shift in pYV PCN but rather for the
443 maintenance of the pYV plasmid in general as it undergoes dynamic shifts in PCN during the
444 *Yersinia* facultative lifestyle. We hypothesize that PAP I polyadenylates and promotes
445 degradation of pYV-encoded CopA sRNA to regulate cellular CopA levels at both 26°C and
446 37°C. This would help maintain CopA levels within a range that promotes maintenance of pYV
447 PCN near its optimal "set point" and ensuring that pYV-encoded gene dosage remains high
448 enough to support replication and maintenance of the plasmid under conditions where pYV PCN
449 is normally kept low. In the absence of PAP I, we hypothesize that pYV plasmid replication rates
450 decrease due to abnormally high CopA sRNA levels, leading to reduced pYV PCN, plasmid
451 stability, T3SS activity, and host tissue colonization.

452

453 We found that PAP I is required for normal *Y. pseudotuberculosis* virulence in a mouse
454 intraperitoneal infection model, consistent with its role in promoting high pYV-encoded gene

455 dosage and pYV stability, and therefore T3SS activity. Interestingly, Δ*pcnB*-infected mice fell
456 into two groups: one in which the spleen and liver were colonized with *Yersinia* to wildtype-
457 infected levels, and another in which no Δ*pcnB* cells could be recovered from spleens and livers
458 four days post-inoculation. Overall, this led to a significant decrease in spleen and liver
459 colonization by Δ*pcnB* compared to wildtype *Y. pseudotuberculosis*. Consistent with our finding
460 that deletion of *pcnB* leads to enhanced pYV loss from the bacterial population *in vitro*, wildtype
461 cultures used for mouse inoculation had 100% retention of pYV whereas the Δ*pcnB* inoculum
462 had an average retention of 81% at the time of inoculation. This 19% decrease in pYV+ Δ*pcnB*
463 cells in the inoculum are not likely to explain the difference in virulence, as wildtype inoculums of
464 10^3 to $3x10^3$ yielded similar spleen and liver colonization levels. These data suggest that
465 *pcnB*/PAP I may aid *Yersinia* surviving a colonization bottleneck during infection. To our
466 knowledge, this is the first time that PAP I has been directly linked to virulence of a bacterial
467 pathogen and highlights the importance of understanding how PAP I and virulence plasmid
468 gene dosage contribute to bacterial pathogenesis. All Δ*pcnB* cells recovered from the spleen
469 and livers of infected mice retained at least one copy of the pYV plasmid despite the plasmid
470 stability defect observed for this strain *in vitro*. These data suggest a selective pressure to retain
471 pYV during growth in mouse tissues, consistent with the importance of the T3SS to *Yersinia*
472 virulence. This contrasts with what we observe *in vitro* when pYV and T3SS expression is a
473 metabolic burden and not a benefit. These data suggest that *pcnB*/PAP I is required for
474 maintenance of the pYV plasmid when pYV is dispensable to survival. This is necessary to
475 ensure that enough of *the Y. pseudotuberculosis* population is pYV^+ to be able to colonize a
476 new host and survive in host tissues.

477

478 In addition to pYV and pINV, we found that *pcnB* is important for robust replication of sRNA-
479 regulated plasmids encoding antimicrobial resistance (AMR) genes in *Yersinia* and *Shigella*.

480 When *Y. pseudotuberculosis* or *S. flexneri* Δ*pcnB* cells are grown in the presence of the
481 plasmid-selective antibiotic, we observed a ten-fold decrease in growth (Fig 5 and 7), consistent
482 with previous studies in *E. coli* [29]. Similarly, we found a ten-fold decrease in GFP fluorescence
483 in the *Y. pseudotuberculosis* Δ*pcnB* strain carrying the ColE1 pGFPuv plasmid compared to
484 wildtype, suggesting a ten-fold decrease in plasmid-encoded gene expression in the absence of
485 *pcnB*. In addition, time course experiments found that the majority of the Δ*pcnB* population loses
486 the pGFPuv plasmid within just 10 hours of removing the selective antibiotic. These data
487 support that ColE1 PCN and plasmid stability are reduced in the absence of PAP I, rendering
488 cells more antibiotic susceptible. Interestingly, the rate at which pYV is lost from *Y.*
489 *pseudotuberculosis in vitro* under non-T3SS inducing conditions was far slower than for
490 pGFPuv. We passaged wildtype and Δ*pcnB* strains in LB medium at 26°C and while 100% of
491 wildtype retained pYV, only ~60% of Δ*pcnB* cells retained pYV by 13 days with a still increasing
492 rate of loss. As pGFPuv has no active plasmid partitioning or maintenance systems but pYV has
493 both ParABS and ParDE systems, we hypothesize that the rate of plasmid loss in cells lacking
494 PAP I activity will depend on the presence and type of plasmid-encoded mechanisms that
495 promote plasmid stability.

496

497 Through our RNA-seq analysis we identified several differentially regulated transcripts in the *Y.*
498 *pseudotuberculosis* Δ*pcnB* mutant that are involved in responding to several types of stress,
499 including the universal stress protein UspB, the *Yersinia* urease operon, and several cold-shock
500 proteins (Supplemental Dataset 1). Importantly, these differentially regulated genes are
501 encoded on the *Y. pseudotuberculosis* chromosome and so should not be significantly affected
502 by the pYV PCN defect in the Δ*pcnB* mutant. In addition, EcPAP from *E. coli* has been
503 previously reported to play a critical role in regulating mRNA transcripts important for
504 responding to stress where loss of PAP I leads to stabilization of stress response transcripts

505 [43]. Deletion of *pcnB* in *E. coli* results in increased tolerance to several stresses, including
506 osmotic stress, acid stress, heat shock, and cold shock [83]. Interestingly, we found that loss of
507 PAP I does not affect *Y. pseudotuberculosis* viability following heat shock, growth at 4˚C, acid
508 shock, or osmotic shock (Fig S7). Our RNA-seq analysis also found that some stress response
509 genes such as CspE are downregulated in Δ*pcnB* cells, suggesting that PAP I normally
510 promotes stability of at least some stress-related transcripts in *Y. pseudotuberculosis*. These
511 data suggest that while PAP I stabilizes sRNA-regulated plasmids in multiple bacterial species,
512 its effect on stress responses is species-specific.

513

514 While *E. coli* EcPAP and PAP I from *Y. pseudotuberculosis* and *S. flexneri* are highly conserved
515 in general, some regions of the proteins are less conserved and might account for their different
516 impacts on stress tolerance. Interestingly, while the PAP I N-terminal region following the initial
517 propeptide sequence is predicted to be disordered, this is also the region that displays the least
518 amount of conservation between the three proteins. In contrast, this N-terminal region is 100%
519 conserved between *Y. pseudotuberculosis* and *Y. pestis* (Fig S8). This disordered region is also
520 significantly expanded in length for PAP I from *Y. pseudotuberculosis* and *Y. pestis* compared to
521 *E. coli* and *Shigella* PAP I (Fig 2A). Given that disordered regions of RNA-binding proteins have
522 been proposed to mediate interactions with target RNAs and/or other proteins [84], it is possible
523 that *Yersinia* PAP I has evolved to target different RNA transcripts and/or interacts with one or
524 more unique protein partners compared to EcPAP. *Yersinia* PAP I complements the plasmid-
525 encoded antibiotic resistance defect of the *Shigella* Δ*pcnB* mutant, suggesting that PAP I plays
526 a conserved role in regulating plasmid-derived sRNAs. However, given the different role of PAP
527 I in stress resistance in *Yersinia* and *E. coli*, PAP I may be adapted to regulate chromosomally-
528 derived mRNA transcripts in a more species-specific way.

529

530 In this study, we show for the first time that *pcnB*/PAP I is required for maintenance of a large
531 IncFII virulence plasmid (pYV) that undergoes dynamic yet specific changes in PCN to regulate
532 virulence gene dosage in *Y. pseudotuberculosis*. PAP I was also found to be required for normal
533 *Y. pseudotuberculosis* virulence, providing the first direct evidence that PAP I regulates
534 virulence of a Gram-negative pathogen. PAP I is required for maintenance of plasmids from
535 multiple families in *Y. pseudotuberculosis* and *S. flexneri* (Fig 5 and 7; Fig S5), including families
536 that commonly include virulence and antimicrobial resistance plasmids. PAP I homologs can be
537 found in many species of Gram-negative pathogenic bacteria, many of which harbor
538 extrachromosomal plasmids important for their pathogenic lifestyles, and genomic studies show
539 that the *pcnB* gene is highly subject to horizontal gene transfer [36]. Our data support the idea
540 that bacterial PAP I has a conserved role in promoting the stability of many sRNA-regulated
541 plasmids and may be critical for the establishment of new plasmids in a bacterial population
542 following horizontal transfer by promoting plasmid replication. However, given the different
543 effects of PAP I loss to stress resistance in *E. coli* and *Yersinia*, PAP I-mediated polyadenylation
544 of transcripts that are chromosomally-encoded likely varies across species. Future studies will
545 explore the possibility of targeting PAP I activity as a novel antibiotic and/or plasmid-curing
546 strategy as well as the contribution of PAPI-mediated polyadenylation to regulation of gene
547 expression in different pathogenic bacteria.

548

549 **Materials and Methods**

550 **Bacterial strains, plasmids, and growth conditions**

551 All strains used in this study are listed in Table S2. *Y. pseudotuberculosis* strains were grown in
552 LB or 2xYT media (pH=7) at 26°C or 37°C shaking at 250rpm, unless otherwise indicated. *S.*
553 *flexneri* were grown in tryptic soy broth media at 30°C or 37°C on a roller.

554

555 **Construction of *Y. pseudotuberculosis* and *S. flexneri* mutant strains**

556 All primers and plasmids used to generate *Y. pseudotuberculosis* strains for this study are listed
557 in Tables S3 and S4, respectively. Inserts were amplified by PCR using primers designed for
558 Gibson Assembly and final recombinant plasmids were all made using the pCVD442 suicide
559 vector backbone (λpir-dependent replicon, carbenicillin resistant [$Carb^R$], *sacB* gene conferring
560 sucrose sensitivity) (Addgene) following digestion with NdeI and BbsI. All ligations were
561 performed using NEBuilder HiFi DNA Assembly kit (New England Biolabs). Recombinant
562 pCVD442 plasmids were transformed into *E. coli* S17-1 λpir competent cells and introduced into
563 Y*. pseudotuberculosis* IP2666pIB1 or YPIII/pIBX via conjugation. $Carb^R$ and irgansan-resistant
564 (*Yersinia* selective antibiotic) clones were grown in the absence of antibiotics and plated onto
565 media containing 10% sucrose to induce SacB-mediate toxicity for pCVD442 loss. Carb
566 sensitive, sucrose-resistant, and Congo red-positive (pYV+) clones were screened by PCR and
567 sequence verified by Sangar sequencing. <u>*pil* insertion strains:</u> A *pil::Tn Y. pseudotuberculosis*
568 IP2666pIB1 ∆yop6 strain was originally isolated from a Tn*Himar1* library screened for altered
569 NFκB induction compared to the parental strain (52). The Tn insertion was then transferred to
570 the wildtype IP2666pIB1 strain using the pSR47s suicide plasmid, as described above. The
571 *pil::pNQ Y. pseudotuberculosis* YPIII/pIBX mutant was generated using the synthesized
572 pNQ705 suicide plasmid carrying a truncated fragment of *pil* (Genescript)[85]. <u>∆*pcnB*:</u> ~500 bp
573 upstream of *pcnB* and ~500 bp downstream of *pcnB* was PCR amplified using genomic DNA
574 (gDNA) from *Y. pseudotuberculosis* IP2666pIB1. Amplified fragments were cloned into
575 pCVD442 to produce pCVD442::∆*pcnB*. <u>ParB-GFP:</u> To make ParB-GFP YPIII/pIBX strains,
576 three fragments were amplified for insertion into pCVD442: (1) the last ~500 bp of the *parB*
577 gene excluding the stop codon was amplified from *Y. pseudotuberculosis* gDNA, (2) msfGFP
578 was amplified from pDK13 and (3) 500 bp downstream of the *parB* gene was amplified from *Y.*

579 *pseudotuberculosis* gDNA. The resulting fragments were cloned into pCVD442 to generate a
580 *parB*-msfGFP construct that includes 500 bp of downstream homology after msfGFP. PAPI-C-
581 6xHis and PAPI-C-3xFLAG: To make PAPI-6xHis strains, *pcnB* was amplified from *Y.*
582 *pseudotuberculosis* gDNA and cloned into pET28 that was previously digested with XhoI and
583 NcoI to produce PAPI-C-6xHis. PAPI-C-6xHis was then amplified from pET28 and 500bp
584 downstream of *pcnB* was amplified from gDNA for insertion into pCVD442 to make
585 pCVD442::PAPI-c-6xHis containing 500 bp of homology flanking the 6xHis tag. We
586 subsequently found that the 6xHis tag was not sufficient to visualize the PAPI protein, and so
587 alternative PAPI-C-3xFLAG strains were made in order to carry out western blot analyses. To
588 make PAPI-3xFLAG, three fragments were amplified for insertion into pCVD442: (1) the *pcnB*
589 gene was amplified from *Y. pseudotuberculosis* gDNA (2) 3xFLAG was amplified from pET28
590 and (3) 300 bp downstream of *pcnB* was amplified from *Y. pseudotuberculosis* gDNA. The
591 fragments were then cloned into pCVD442 to make pCVD442::PAPI-c-3xFLAG containing 300
592 bp of downstream homology following the 3xFLAG tag. PAP 1 point mutations: To make PAP
593 I^{D2A}, PAP I^{L291R}, and PAP I^{L291A} mutants, we used the Q5 site-directed mutagenesis kit (New
594 England Biolabs) to introduce base pair changes at the corresponding residues using the
595 pCVD442::PAPI-c-6xHis or pCVD442::PAPI-c-3xFLAG recombinant plasmids as templates.
596 *ΔipaH2.5ΔpcnB Shigella:* A fragment containing 200 bp of homology upstream and 240bp of
597 downstream *pcnB* flanking sequence was amplified from ECK0142 (*ΔpcnB E. coli* K-12
598 BW25113) (PMID 16738554) using pcnb_F and pcnb_R. This fragment was introduced into the
599 chromosome of *ΔipaH2.5::tetR Shigella* (PMID: 25378474) using lambda red recombination
600 (PMID: 10829079). The insertion was confirmed using pcnB_R_op and k2_wanner.

601

602 ***In vitro* suppressor screen**

603 LB cultures of the *pil::*pNQ YPIII/pIBX mutant strain were grown at 26ºC shaking overnight

604 before diluting in fresh media and spotting for single colonies onto low calcium plates (LB
605 supplemented with 20 mM sodium oxalate and 20 mM $MgCl_2$). Plates were incubated at 37ºC
606 for ~16 hours to induce T3SS expression and selective pressure for growth of suppressor
607 mutants. Clones that broke growth arrest and thus formed large colonies were selected and
608 screened for changes in pYV PCN using the luciferase assay (see below). Suppressor mutants
609 were also screened for changes in T3SS activity using an *in vitro* secretion assay (see below).

610

611 **Identification of mutations arising from *pil::*pNQ suppressor screen**

612 A subset of *pil::*pNQ YPIII/pIBX suppressor mutants were selected for whole genome
613 sequencing. In brief, cells were grown shaking at 26ºC overnight and total genomic DNA was
614 extracted using the Blood & Tissue DNeasy kit (Qiagen) according to manufacturer
615 recommendations. Qubit quantification, library preparation, and Illumina paired-end sequencing
616 with 150 bp read length was carried out by the UC Davis DNA Technologies Core. Adapters and
617 low-quality reads were trimmed by Trimmomatic (Version 0.39)[86]. The trimmed sequences
618 from each sample were aligned to the reference genome using BWA [87] The reference
619 sequence was composed of the YPIII chromosome (CP009792.1) [88] and its plasmid
620 (CP032567.1)[89]. Samtools [90] was used to sort and index the aligned reads. Duplicate reads
621 originated from a single DNA fragment during sample preparation were located and tagged by
622 MarkDuplicates in Picard (http://broadinstitute.github.io/picard/). Single nucleotide
623 polymorphisms were detected and joined by GATK (Version 4.1.6) [91].

624

625 **Droplet digital PCR (ddPCR)**

626 ddPCR to determine pYV plasmid copy number was carried out as previously described [92].
627 Total DNA was extracted from bacterial cells using GeneJet Genomic DNA Purification kit

628 (Thermo Scientific) according to the manufacturer's recommendations for Gram-negative
629 bacteria. Each genomic DNA sample was split into two reactions and the primer pair
630 F_chrom_ddPCR/R_chrom_ddPCR was used for to amplify chromosomal DNA and
631 F_pYV_ddPCR/R_pYV_ddPCR was used to amplify pYV DNA. Individual ddPCR samples were
632 prepared as follows: 10.5 µL of total genomic DNA was combined with 12.5 µL of 2xEVA-Green
633 master mix for unlabeled probes (Bio-Rad), 1 µL of HindIII-HF (NEB), and 1 µL of respective
634 primer pairs (200 nM final concentration) in 8-strip PCR tubes. PCR tubes were incubated at
635 room temperature for 10 minutes to allow HindIII to digest genomic DNA. Droplet generation
636 was carried out using an Automated Droplet Generator (Bio-Rad) and droplets were
637 subsequently transferred to a deep-dish qPCR plate (Bio-Rad) for PCR amplification. PCR was
638 carried out with hot-start activation at 95°C for 5 mins following by denaturation at 94°C for 30s,
639 amplification at 58°C for 1 min over 40 cycles, and signal stabilization at 4°C for 10 min and
640 90°C for 5 min. A ramp rate of 2C/s was used for all PCR steps. Droplets were analyzed using a
641 QX200 droplet reader (Bio-Rad) and data was analyzed using QuantaSoft Analysis Standard
642 Edition (version 1.2) (Bio-Rad). Statistical significance was calculated using a one-way ANOVA
643 with Tukey's multiple-comparisons test (**** $P<0.0001$, *** $P<0.001$, ** $P<0.01$, * $P<0.05$). All
644 graphs and statistical analyses were generated using GraphPad Prism (10.2.0).

645

646 **Luciferase pYV plasmid copy number assay**

647 Overnight cultures for strains in the YPIII/pIBX background were grown shaking at 26ºC before
648 subculturing to an OD_{600} of 0.2 in 2xYT low calcium media (containing 20mM sodium oxalate
649 and 20mM $MgCl_2$). Cultures were then grown shaking for 1.5h at 26ºC before shifting to 37ºC.
650 Luminescence and OD_{600} were measured after 1.5h at 26ºC just before shifting to 37ºC and
651 every hour after shifting to 37ºC. Samples were collected at each timepoint in white walled,
652 clear bottom 96 well plates and luminescence (using lum aperture for 96 well plate with

653 measurement time=0.1s) and OD_{600} (using Photometric 600 excitation filter) was measured
654 using a PerkinElmer Multimode Plate Reader EnVision system. Relative plasmid copy number
655 was determined by dividing luminescence by OD_{600} for the same sample. Statistical analysis
656 was determined using a one-way ANOVA with Dunnett's multiple comparisons test (****
657 P<0.0001, *** P<0.001, ** P<0.01, * P<0.05) where applicable. All graphs were made using
658 GraphPad Prism (10.2.0).
659

660 **ParB-msfGFP microscopy and image analysis**

661 Wildtype and Δ*pcnB* YPIII/pIBX cells expressing ParB-msfGFP from LB plates supplemented
662 with kanamycin were inoculated into EZ Rich Defined Medium (EZRDM) (Teknova) without
663 antibiotic supplementation. EZRDM medium was chosen to reduce medium autofluorescence
664 for downstream imaging purposes. Cultures were grown shaking at 200 rpm overnight at 26ºC
665 to a final OD_{600} of ~2-4. A secretion analysis was performed to confirm that *Y.*
666 *pseudotuberculosis* displays normal T3SS activity when grown in EZRDM under T3SS-inducing
667 conditions (37°C, supplemented with 20 mM sodium oxalate and 20 mM $MgCl_2$), referred to as
668 low calcium EZRDM (Fig S9). For non-T3SS inducing conditions, overnight cultures were
669 diluted to an OD_{600} of ~0.2 in fresh EZRDM and grown shaking for 3 hours at 26ºC. For T3SS-
670 inducing conditions, overnight cultures were diluted to an OD600 of ~0.2 in low calcium EZRDM
671 and grown shaking for 1.5 hours at 26ºC before shifting to 37ºC for an additional 1.5 hours.
672 Cells were prepared for imaging by spotting onto a 1% agarose-low calcium EZRDM pad and
673 covering with a no. 1.5 coverslip. Imaging was carried out using a Nikon Eclipse Ti microscope
674 equipped with a 100X Plan Apo 1.45 NA phase-contrast oil objective, a Hamamatsu Orca-
675 Flash4.0 V2 CMOS camera, and CoolLED pE-400 (Lumencor). The microscopes were
676 controlled by the Nikon Elements software. The following Chroma filter cubes were used to
677 acquire the fluorescence images: GFP: excitation ET470/40x, dichroic T495lpxr, emission

678 ET525/50 m. Images were acquired with 50 ms of exposure (50% power) for GFP and 100 ms
679 for phase contrast. For each strain and condition, three independent biological replicates
680 (inoculated with different colonies) were grown and imaged.

681 For image analysis, cells were segmented and cell outlines were generated using the open-
682 source Oufti software [93] using the following parameters: Edgemode, 1; Dilate, 1; openNum, 0;
683 InvertImage, 0; ThreshFactorM, 0.86254; ThreshMinLevel, 0.3; EdgeSigmaL, 0.5; LogThresh,
684 0. Cell meshes were further curated using the SVMCuratedCellDetection.m script to identify and
685 remove misdetected cells [94]. To quantify the number of pYV copies per cell, detection of pYV
686 spots was performed using the ImageJ plug-in package ThunderSTORM [95, 96]. For of cells
687 grown at 26ºC, image filtering used a wavelet filter (B-spline) with a scale of 2.0 and order of
688 3.0. Under non-T3SS-inducing conditions, a local maximum using 5.0*std(Wave.F1) and a
689 connectivity of 8-neighborhood was used to localize molecules based on peak intensity
690 thresholds, and sub-pixel localization used a Gaussian point spread function (PSF) with a fitting
691 radius of four pixels and an initial sigma of one pixel. For the 37ºC/low calcium condition, the
692 parameters were adjusted where the local maximum instead used 2.0*std (Wave.F1) and a
693 connectivity of 8-neighborhood, and sub-pixel localization used a Gaussian PSF with a fitting
694 radius of three pixels and an initial sigma of one pixel. Once parameter optimization was
695 completed, the custom-made ImageJ macro BatchProcess_ThunderSTORM,ijm was used to
696 iterate ThunderSTORM spot detection over all image files, applying the same parameters for a
697 given biological replicate. Detected spots were linked with cell meshes using the custom
698 MATLAB code analyze_ensemble_spot_intensity.m, detailed further below. Code developed as
699 part of this study has been deposited in the publicly accessible Github code repository
700 (https://github.com/JacobsWagnerLab/published/tree/master/Schubert_et_al_2024). Three
701 independent experiments were performed and analyzed per strain and condition.

702 Elaborating on the MATLAB script analyze_ensemble_spot_intensity.m, each cell was
703 quantified by averaging whole cell intensity, recording the number of ThunderSTORM-detected
704 spots, and noting the cell length. Only cells with length of at least 1μm were kept to rule out
705 incorrect cell segmentations. Each cell was identified and measured from its original Oufti mesh.
706 There, the fluorescent GFP images were background-subtracted, then cell contours were used
707 to obtain the boundaries of the cell area. Cellular fluorescence was determined by Oufti [93]. To
708 link ThunderSTORM spots, (*x*,*y*) localizations, to Oufti meshes, the cell meshes were first
709 converted to MATLAB polygons using the function *polyshape*. The function *inpolygon* was then
710 used to feed the (*x*,*y*) localizations and polygon shape to find if any spots occurred inside the
711 cell. For Fig 3 C-E, cells with zero spot were excluded from the analysis.

712 To assess what fraction of cells were devoid of GFP signal, strains were grouped by condition
713 (inducing vs. non-inducing as 37ºC/low calcium vs. 26ºC, respectively). Each strain in the
714 condition was subsetted by random sampling without replacement to match the lowest N value
715 (7,033 cells in 26ºC and 10,003 cells in 37ºC/low calcium) using the function *datasample*. These
716 data were then bootstrapped 100 times to recalculate histograms and determine the error for
717 each bin (using the custom function *Hist_Errors*). Since the Δ*pcnB* conditions had clear bimodal
718 distributions for low/high fluorescent states, an Otsu threshold was calculated using the function
719 *otsuthresh* to find the split between them [97]. Cell with intensity values below this threshold
720 were deemed cells without plasmid content. To compare these two distribution shapes
721 statistically, a Kolmogorov-Smirnov (KS) test was used via the function *kstest2*.

722 Images were visualized using NIS Elements and Fiji. Image pixel intensity values were auto-
723 scaled for display using Fiji, and all images were converted to RGB format for display. Data
724 were plotted using GraphPad Prism 10.2.0, and Adobe Illustrator was used to generate figures.

725

726 ***In vitro* pYV plasmid stability assay**

727 Cells were struck for single colonies onto LB plates and grown at 26°C for 1.5-2 days. To test
728 plasmid stability after 26°C-only passage, single colonies were then patched onto LB plates for
729 ~16 hours at 26°C before heavily streaking for single colonies onto fresh LB plates at 26°C for
730 1.5-2 days. To test plasmid stability after exposure to T3SS-inducing conditions (37˚C), the
731 same colonies were also patched onto LB plates supplemented with 20 mM sodium oxalate to
732 induce T3SS activity for ~16 hours at 37ºC before streaking for single colonies onto LB plates
733 and returning to 26ºC to grow for 1.5-2 days. Final plasmid stability was determined for both
734 conditions by patching single colonies from the final 26°C streak on LB plates supplemented
735 with 20 mM sodium oxalate and containing 1% Congo red. The percentage of cells that retained
736 the pYV plasmid was calculated by dividing the number of red (pYV+) CFU by the total number
737 of CFU. Single colony PCR was used on a subset of patches to validate that red CFU retain
738 pYV and while white CFU do not.

739

740 ***In vitro* T3SS activity assay**

741 Quantification of secreted *Yersinia* T3SS cargo was carried out as previously described [98]. *Y.*
742 *pseudotuberculosis* cultures were grown shaking overnight at 26°C before subculturing in LB
743 low calcium media (LB containing 20 mM sodium oxalate and 20 mM $MgCl_2$). Cultures were
744 grown shaking at 26°C for 1.5 hours before shifting to 37°C/shaking for an additional 1.5 hours.
745 Cultures were normalized to the same number of cells by normalizing OD_{600} values and pelleted
746 at 13,200 rpm for 15 min at room temperature. Supernatants were transferred to new tubes and
747 proteins precipitated with 10% trichloroacetic acid (TCA). A bovine serum albumin (BSA) protein
748 control was spiked into each sample immediately before the addition of TCA. Samples were
749 incubated in TCA on ice for at least 1h before pelleting at 13,200 rpm for 15 min at 4°C. Pellets
750 were then washed twice with ice-cold 100% acetone and resuspended in final sample buffer

751 (FSB) containing 0.2M dithiothreitol (DTT). Samples were boiled for 10 min at 95°C before
752 loading and separating on a 12.5% SDS-PAGE gel. Gels were stained with Coomassie blue to
753 visualize proteins and imaged using Bio-Rad Image Lab Software Quantity and Analysis tools.

754

755 ***Shigella* T3S secretion assay**

756 *S. flexneri* cultures were grown with shaking overnight in tryptic soy broth (TCS) media with 15
757 µg/mL tetracycline and 50 µg/mL kanamycin at 37°C. In the AM, the cultures were sub-cultured
758 in TCS and grown for 2.5 hours with shaking at 37°C to reach OD_{600} ~1. Cultures were
759 normalized to the same number of cells based on the OD_{600} and pelleted at 13,000 rpm for 1
760 min before resuspending in PBS and 10 µM Congo red and incubated for 30 min shaking at
761 37°C. Pellets and supernatants were separated by centrifugation and supernatants were
762 transferred to new tubes and precipitated with 10% TCA. Supernatant samples were incubated
763 on ice and subsequently pelleted at 15000 rpm for 15 min at 4°C. Pellets were then washed with
764 ice-cold 100% ethanol and resuspended in 1x loading dye buffer with 5% beta-mercaptoethanol.
765 Samples were boiled for 10 min at 95°C before loading on a 12% SDS-PAGE gel for western
766 blot analysis.

767

768

769 **RNA isolation and RNA-seq analysis**

770 *Y. pseudotuberculosis* IP2666pIB1 strains were grown in 3 mL LB overnight at 26°C and diluted
771 the following morning to an OD_{600} of 0.2 in 5 mL fresh LB. Each strain was diluted into two
772 separate cultures (one for each temperature). For 26°C samples, cultures were diluted in plain
773 LB media and grown shaking at 26°C for 3h before extracting RNA. For 37°C samples, cultures
774 were diluted into LB low calcium media (containing 20mM sodium oxalate and 20mM $MgCl_2$)

775 and grown shaking at 26°C for 1.5 hours before shifting to 37°C to growing shaking for an
776 additional 1.5 hours. After incubating, 1-2mL of each culture was collected and pelleted for 5
777 min at 4,000 rpm. Supernatants were removed and cell pellets were resuspended in 1mL RNA
778 Protect (Qiagen) and total RNA was isolated using the RNeasy minikit (Qiagen) according to the
779 manufacturer's protocol. DNA was removed from samples using the TURBO DNA-free kit (Life
780 Technologies/Thermo Fischer) and RNA quality was determined using an Agilent 2000
781 Bioanalyzer. Samples were DNase treated with Invitrogen DNase. Library preparation was
782 performed using Illumina's Stranded Total RNA Prep Ligation with Ribo-Zero Plus kit and 10 bp
783 IDT for Illumina indices. Sequencing was done on a NovaSeq 6000 giving 2x51bp reads.
784 Demultiplexing, quality control, and adapter trimming was performed with bcl-convert (v4.0.3).
785 Read mapping was performed with HISAT2 [99]. Read quantification was performed using
786 Subread's featureCounts functionality [100]. Read counts were normalized using edgeR's
787 Trimmed Mean of M values (TMM) algorithm (Supplementary Dataset 1)[101]. Subsequent
788 values were then converted to counts per million (cpm). Differential expression analysis was
789 performed using edgeR's exact test for differences between two groups of negative-binomial
790 counts with an estimated dispersion value of 0.1. Genes for which the $|logFC| > 1$ and $p < 0.05$
791 were considered differentially expressed (Supplementary Dataset 1).

792

793 Heatmaps for pYV-encoded genes were generated using average TMM values via ClustVis
794 [102]. RNA-Seq data are available for viewing, and the track hub data can be found
795 at http://lowelab.ucsc.edu/hubs/yersinia_pcnB_pil_expression/hub.txt on the UCSC Microbial
796 Genome Browser. For these data, chromosomal reads were normalized separately from pYV-
797 encoded reads due to differences in pYV PCN among samples. For this analysis, raw paired
798 reads were aligned to the *Y. pseudotuberculosis* IP2666pIB1 genome (ASM381434v1) using
799 Bowtie2 (v.2.3.5.1) with default options. Bam files were further processed to remove PCR

duplicates using samtools (v1.15.1) as follows, samtools sort -n {input_bam} | samtools fixmate -m - - | samtools sort - | samtools markdup -r - - | samtools view -bq 10 -f 0x1 - > {output_bam}. Finally, bamCoverage-deeptools (v3.5.4) was used to normalize the chromosomal read counts using the following options: --normalizeUsing CPM --ignoreForNormalization NZ_CP032567.1 --outFileFormat bedgraph --binSize 1 --region NZ_CP032566.1. For the non-normalized pYV reads we used bamCoverage-deeptools with options --ignoreForNormalization NZ_CP032566.1 --outFileFormat bedgraph --binSize 1 --region NZ_CP032567.1. Finally, the separate bedgraph files were concatenated and converted to bigwig format using bedGraphToBigWig (v4) with default options.

Western blot analysis

Cells were grown at the indicated temperature before preparing samples for western blotting. Samples were normalized to the same number of cells using OD_{600} at the time of sample collection. Bacterial pellets were then resuspended in FSB containing 0.2M DTT and boiled at 95°C for 15 minutes. Secreted proteins were precipitated using TCA in the same way as described for the *in vitro* secretion assay above. The same volume of each sample was separated on a 12.5% SDS-PAGE gel and proteins were transferred to a blotting membrane (Immunobilon-P) using a wet mini trans-blot cell (Bio-Rad) at 4°C. Blots were blocked for one hour in Tris-buffered saline containing Tween 20 and 5% milk. Blots were probed with anti-RpoA (gift from Melanie Marketon), goat anti-YopE (Santa Cruz Biotech), mouse M2 anti-FLAG (Sigma), and horseradish peroxidase-conjugated secondary antibodies (Santa Cruz Biotech). Bands were visualized using a BioRad ChemiDoc and quantification analysis was performed using Image Lab software (Bio-Rad).

For *S. flexneri* strains, samples were separated by a 12% SDS-PAGE gel and transferred to a nitrocellulose membrane. Blots were probed with anti-IpaB, anti-IpaC, and anti-IpaD antibodies,

825 and anti-rabbit secondary antibodies. Bands were visualized using SuperSignal West Pico
826 PLUS Chemiluminescent Substrate on an Azure 300 Imager.

827

828 **Mouse Infections**

829 C57BL/6 mice were purchased from Jackson Laboratory. Six- to eight-week-old C57Bl/6 mice
830 were infected with 1-3x10^3 *Y. pseudotuberculosis* via intraperitoneal (IP) injection as previously
831 described [103]. In brief, LB overnight cultures of *Y. pseudotuberculosis* were grown shaking at
832 26ºC before spinning down at 5000 rpm and resuspending in sterile PBS (pH 7.4). CFU used for
833 the inoculum cultures were confirmed to contain pYV prior to infection using single colony PCR
834 with primers specific to the pYV plasmid. Samples were then diluted in PBS such that 100 µL
835 contained 1-3x10^3 cells. Inoculums were plated to confirm the inoculation dose and to estimate
836 the percentage of cells that were pYV+ by patching onto LB plates supplemented with 20 mM
837 sodium oxalate and containing 1% Congo red dye. The plasmid retention of the starting
838 inoculums was found to be 100% for wild type and 81% on average for Δ*pcnB*. Mice were
839 injected with 100 µL of inoculum and spleens and livers harvested four days post-inoculation.
840 Organs were homogenized and serial dilutions of the homogenate plated to determine CFU per
841 gram (CFU/g) of tissue.

842

843 **Construction of PAP I expression vector**

844 The *pcnB* ORF was PCR amplified from *Y. pseudotuberculosis* genomic DNA using the primer
845 pair FpcnB_pTrc/RpcnB_pTrc and ligated into pTrc99a previously digested with NcoI and XbaI
846 using NEBuilder HiFi DNA Assembly kit (New England Biolabs, Inc.). Constructs were
847 transformed into DH5α *E. coli* for propagation and sequence verified via Sangar sequencing.
848 The resulting pTrc99a::PAPI recombinant expression vector was introduced to wildtype and
849 Δ*pcnB Y. pseudotuberculosis* by electroporation and selection on LB plates containing

850 carbenicillin. Expression of PAPI was induced by plating onto LB plates containing 0.2 mM
851 IPTG.

852

853 **Spot tests to analyze antibiotic resistance conferred by pGFPuv, pTrc99, and pNF06**

854 Wildtype and Δ*pcnB Y. pseudotuberculosis* IP2666pIB1 were electroporated with 1 µL of
855 pGFPuv [Carb^R] (Gifted by Dr. Manel Camps), pTrc99a, or pNF06::ccdAB [Kan^R] (Gifted by Dr.
856 Laurence Van Melderen) and single colonies were selected by plating on LB plates containing
857 carbenicillin (pGFPuv, pTrc99a) or kanamycin (pNF06). For spot test dilution series analyses,
858 overnight cultures were grown at 26°C in the presence of antibiotics before diluting in PBS (pH
859 7.4) and making a series of 1:10 dilutions. Serial dilutions were spotted onto LB plates
860 containing no antibiotic or LB plates containing the selective antibiotic and plates were
861 visualized after 1-1.5 days of growth at 26°C.

862 Δ*ipa2.5::tet^R* and Δ*ipa2.5*Δ*pcnB S. flexneri* M90Twere electroporated with pTrc99a, and single
863 colonies were selected by plating on LB plates containing ampicillin. For spot tests, overnight
864 cultures were grown at 30°C in the presence of antibiotics before diluting in PBS (pH 7.4) and
865 making a series of 1:10 dilutions. Serial dilutions were spotted onto LB plates containing no
866 antibiotic or LB plates containing the selective antibiotic and plates were visualized after 1 day
867 of growth at 30°C.

868

869 **pGFPuv plasmid loss curve**

870 Wildtype and Δ*pcnB Y. pseudotuberculosis* IP2666pIB1 lacking pYV (pYV-) were electroporated
871 with pGFPuv as described above. Overnight cultures were grown at 26˚C in the presence of
872 carbenicillin. Overnight cultures were diluted 1:1000 into LB media without antibiotics to allow
873 loss of the plasmid. To assess plasmid retention at each timepoint, aliquots of the cultures were

874 plated onto LB agar and incubated at 26˚C. Fifty single colonies from each sample were
875 patched onto LB agar containing carbenicillin. Percentage of plasmid retention was calculated
876 as the number of patched colonies able to grow in the presence of carbenicillin relative to the
877 total number of patched colonies.

878

879

880 **Acknowledgments**

881 We would like to acknowledge Dr. Manel Camps (UC Santa Cruz) for providing the pGFPuv
882 plasmid as well as general advice and guidance on this work. We would also like to
883 acknowledge Dr. Laurence Van Melderen (Université Libre de Bruxelles) for providing us with
884 the pNF06::empty and pNF06::*ccdAB* constructs. Finally, we would like to thank Dr. Petra
885 Dersch (Universität Münster) for providing general advice and technical support for this project.

886

887 **Funding:** This study was supported by National Institutes of Health (www.NIH.gov) grant
888 R01AI141511 (to VA), R01AI128360 (to CFL), and the Swedish Research Council 2018-02376
889 and 2022-00741 (to HW). CJW is an investigator of the Howard Hughes Medical Institute. HNL
890 was supported by NIH K99AI139281. KS was supported by an NIH T32 GM008646 training
891 grant. The funders had no role in study design, data collection and analysis, decision to publish,
892 or preparation of the manuscript.

893

894 **Competing interests:** The authors have declared that no competing interests exist.

895

896 **Figure Legends**

897 **Figure 1. *Y. pseudotuberculosis* pYV plasmid copy number (PCN) dynamically changes**
898 **in response to temperature. (A)** pYV plasmid copy number per chromosome was determined
899 for wildtype *Y. pseudotuberculosis* IP2666pIB1 grown at 26°C or 37°C/low calcium using droplet
900 digital PCR (dd)PCR. **(B)** Relative pYV plasmid copy number of wildtype *Y. pseudotuberculosis*
901 YPIII/pIBX was determined following growth at 26°C or 37°C/low calcium using a luciferase
902 reporter stably incorporated in the pIBX plasmid, normalized to bacterial cell density (OD_{600}). (A-
903 B) Averages of three independent experiments are shown ± standard deviation (Student t-test,
904 *** $p<0.001$, ** $p<0.01$, * $p<0.05$). **(C)** Representative phase contrast (left) and fluorescence
905 (right) images of *Y. pseudotuberculosis* YPIII/pIBX cells where the pYV plasmid is visualized
906 using a ParB-msfGFP fluorescent marker. Images are shown for cells grown at 26°C or under
907 the 37°C/low calcium condition. **(D)** Histogram depicting the number of ParB-msfGFP-labeled
908 puncta of pYV quantified from data illustrated in panel C. Three biological replicates per
909 condition were imaged and analyzed; for each strain and condition, between 790 to 4428 cells
910 were analyzed per replicate.

911

912 **Figure 2. Disruption of the *pcnB* gene encoding poly(A) polymerase PAP I decreases pYV**
913 **PCN as well as T3SS expression and activity. (A)** PAP I from *Y. pseudotuberculosis*
914 IP2666pIB1, *E. coli* K12, and *S. flexneri* M90T are highly conserved. Known PAP I domains
915 include the head domain (blue), the neck domain (green), the body domain (purple), and the leg
916 domain (yellow) [62]. Residues in boxes represent known catalytic residues from EcPAP and
917 the residue indicated with an arrow represents the residue that was mutated in the L291R *pcnB*
918 suppressor mutants. **(B)** pYV plasmid copy number per chromosome was determined for *Y.*
919 *pseudotuberculosis* IP2666pIB1 strains grown at 26°C or 37°C/low calcium using ddPCR.
920 Averages of three independent experiments are shown ± standard error of the mean. Statistical
921 significance was calculated using a one-way ANOVA with Tukey's multiple comparisons test

922 (**** p<0.0001, *** p<0.001, ** p<0.01, * p<0.05). **(C)** *Y. pseudotuberculosis* IP2666pIB1 strains
923 were grown in low calcium media at 37°C before preparing samples for western blotting.
924 Bacterial pellets were collected and secreted proteins (Yops) were precipitated from the
925 supernatant (sup). Images shown represent a single blot that was independently probed for
926 YopE and RpoA, which serves as a loading control.

927

928 **Figure 3. The *pcnB* gene is required for maintenance of the pYV plasmid. (A)**
929 Representative phase contrast (left) and fluorescence (right) images of *Y. pseudotuberculosis*
930 YPIII/pIBX Δ*pcnB* cells where the pYV plasmid is visualized using a ParB-msfGFP fluorescent
931 marker. Images are shown for cells grown at 26°C or under the 37°C/low calcium condition.
932 White arrowheads indicate plasmidless cells. **(B)** Histograms comparing wildtype vs. Δ*pcnB*
933 cells under 26°C or 37°C/low calcium conditions. Mean fluorescence intensity values are plotted
934 on the x-axis ($\log_{10}$). Shaded error bars represent the mean ± standard error of the mean from
935 bootstrapping the data 100 times. Both histograms were randomly sampled without replacement
936 to match the lowest n value of either condition (7,003 and 10,033 for the 26ºC and 37ºC/low
937 calcium conditions, respectively). Both distributions are significantly different ($p < 10^{-100}$) by
938 Kolmogorov-Smirnov tests. A.U. indicates arbitrary units. **(C)** Histograms depicting the number
939 of ParB-msfGFP-labeled puncta of pYV quantified from data illustrated in panel A. Only cells
940 with at least one detected pYV spot were considered. Three biological replicates were imaged
941 and analyzed per condition. For each strain and condition, between 2063 to 14,479 cells were
942 analyzed per replicate. **(D)** Same as (C) except that the comparison is between wildtype and
943 Δ*pcnB* cells grown at 26°C. For each strain and condition, between 760 to 4179 cells were
944 analyzed per replicate. **(E)** Same as (D) except for the 37°C/low calcium condition. For each
945 strain and condition, between 2046 to 14,479 cells were analyzed per replicate. Distributions in
946 panels D and E are significantly different ($p < 10^{-80}$) by Kolmogorov-Smirnov tests.

947

948 **Figure 4. PAP I point mutations lead to a decrease in pYV PCN, plasmid stability, and**
949 **T3SS activity. (A)** *Y. pseudotuberculosis* IP2666pIB1 strains harboring various PAP I^{FLAG}
950 alleles grown at 26°C or 37°C/low calcium were pelleted and prepared for western blot
951 analyses. Images shown represent a single blot that was cut after transferring and
952 independently probed for expression of PAP I^{FLAG} (top) and RpoA (loading control, bottom).
953 Data shown is representative of three biological replicates. **(B)** *Y. pseudotuberculosis*
954 IP2666pIB1 strains were grown at 26°C before diluting and spotting onto either LB or low
955 calcium plates containing Congo red dye and incubated at 26°C or 37°C, respectively, prior to
956 imaging. **(C)** Relative pYV plasmid copy number was estimated for strains in the *Y.*
957 *pseudotuberculosis* pIBX/YPIII background. For each timepoint, luminescence was measured
958 and normalized to cell density (OD_{600}). Averages of three independent experiments are shown ±
959 standard error of the mean. Each strain per condition was compared to the wildtype (WT) strain
960 in a one-way ANOVA with Dunnett's multiple comparisons test (**** P<0.0001, *** P<0.001, **
961 P<0.01, * P<0.05). **(D)** *Y. pseudotuberculosis* IP2666pIB1 strains were grown at 37°C/low
962 calcium and secreted proteins in the supernatant fractions were precipitated and visualized after
963 separation on as SDS-PAGE gel by Coomassie blue staining. Bovine serum albumin (BSA) was
964 used as a loading and protein precipitation control. The YopE T3SS effector protein band from
965 four independent experiments was visualized, quantified, and normalized to BSA from the same
966 samples. Bars represent the mean fold change in YopE/BSA relative to wildtype and error bars
967 represent the standard error of the mean between different experiments. Statistical significance
968 was determined using a one-way ANOVA with Dunnett's multiple comparisons test (****
969 P<0.0001, *** P<0.001, ** P<0.01, * P<0.05).

970

971 **Figure 5. The *pcnB* gene is required for plasmid-mediated antibiotic resistance in**
972 ***Y. pseudotuberculosis.* (A)** Wildtype and Δ*pcnB Y. pseudotuberculosis* IP2666pIB1 harboring
973 pGFP-uv were spotted simultaneously onto either plain LB plates or LB plates containing
974 carbenicillin to assess retention of pGFP-uv. Plates were incubated at 26°C for ~16 hours
975 before imaging spots under a GFP filter. **(B)** Retention of the pGFP-uv plasmid by wildtype and
976 Δ*pcnB Y. pseudotuberculosis* IP2666pIB1 was assessed at 26°C over 40 hours following the
977 removal of carbenicillin. **(C)** Wildtype and Δ*pcnB Y. pseudotuberculosis* IP2666pIB1 harboring
978 either no vector, a pTrc99::empty vector control, or a pTrc99::PAP I recombinant plasmid were
979 spotted onto either plain LB plates or LB plates containing carbenicillin to select for pTrc99 and
980 0.2 mM IPTG to induce PAP I expression. Plates were incubated at 26°C for ~16 hours prior to
981 imaging. **(D)** Wildtype and Δ*pcnB Y. pseudotuberculosis* IP2666pIB1 harboring either no vector
982 or a pNF06 mini-F plasmid with a *ccdAB* TA system (pNF06::*ccdAB*) were spotted onto either
983 plain LB plates or LB plates containing 25 µg/mL kanamycin to select for pNF06. Plates were
984 incubated at 26°C for ~16 hours prior to imaging.

985

986 **Figure 6. The *pcnB* gene is required for normal *Y. pseudotuberculosis* virulence in a**
987 **mouse IP infection model.** Six- to eight-week-old C57Bl/6 mice were infected with 1-3x10^3 *Y.*
988 *pseudotuberculosis* IP2666pIB1 via intraperitoneal (IP) injection. Tissues were collected,
989 homogenized, and plated to determine CFU per gram (CFU/g) tissue 4 days post-inoculation.
990 The $\log_{10}$ CFU/g tissue from the spleens **(A)** and livers **(B)** of infected mice are shown. Each
991 circle represents one mouse organ; lines represent geometric means.

992

993 **Figure 7. The *pcnB* gene is required for plasmid-encoded expression of T3SS and**
994 **antibiotic resistance genes in *Shigella flexneri*. (A)** *S. flexneri* M90T Δ*ipaH2.5* and

995 Δ*ipaH2.5*Δ*pcnB*, as well as a virulence plasmid cured (VP$^-$) BS103 strain, were incubated on
996 Congo red media at 37˚C. **(B)** *S. flexneri* M90T Δ*ipaH2.5* and Δ*ipaH2.5*Δ*pcnB* carrying pTRC99
997 with and without IPTG-inducible *Yersinia* PAP I were incubated at 37˚C, and secreted T3SS
998 effector proteins were visualized after separation on as SDS-PAGE gel using anti-IpaB, anti-
999 IpaC, and anti-IpaD antibodies. **(C)** *S. flexneri* M90T Δ*ipaH2.5* and Δ*ipaH2.5*Δ*pcnB* carrying
1000 pTRC99 with and without IPTG-inducible *Yersinia* PAP I were grown on either plain TCS media
1001 or TCS containing ampicillin and IPTG. Shown is one of two independent experiments.

1002

1003

1004

1005 **Supporting Information**

1006

1007 **Figure S1. A transposon insertion into *pil* leads to a constitutively high pYV PCN,**
1008 **elevated T3SS expression, and a severe growth defect under T3SS-inducing conditions.**
1009 **(A)** HEK293T cells expressing an NFκB luciferase reporter were left uninfected (uninf) or were
1010 infected with an effectorless Δyop6 strain (Δ*yopHEMOJ*), a Δ*yscNU* T3SS-deficient strain, or
1011 *pil::Tn* in the *Y. pseudotuberculosis* IP2666pIB1 background. Averages of three independent
1012 replicates ± standard error the mean are shown (Student t-test, $p<0.04$). **(B)** Schematic
1013 representation of the location of *pil*. The *pil* locus is located ~123bp away from the *copB* gene.
1014 **(C)** Wildtype, *pil::Tn*, and Δ*pil* IP2666pIB1 were grown at 37°C/low calcium and secreted T3SS
1015 cargo proteins (Yops) were precipitated and visualized by Coomassie blue staining. Bovine
1016 serum albumin (BSA) serves as a loading and precipitation control. Data shown is
1017 representative of three independent replicates. **(D-E)** Relative pYV PCN was estimated for
1018 strains in the YPIII/pIBX background of *Y. pseudotuberculosis* using a luciferase plasmid copy
1019 number assay. For each timepoint, luminescence was measured and normalized to cell density

1020 (OD_{600}). Representative data from three independent experiments are shown. **(E)** Serial
1021 dilutions for wildtype YPIII/pIBX and the *pil*::pNQ congenic *Y. pseudotuberculosis* strains were
1022 spotted onto low calcium agar plates for ~16 hours at 37°C before imaging. The yellow arrow
1023 indicates an example of a large colony in the *pil*::pNQ mutant background that represents a
1024 candidate suppressor mutant.

1025

1026 **Figure S2. T3SS gene mRNA levels are higher in the *pil*::Tn mutant and lower in the**
1027 **Δ*pcnB* mutant compared to wildtype.** Heat maps displaying relative expression of pYV-
1028 encoded genes from RNA-seq analysis of *Y. pseudotuberculosis* IP2666pIB1 strains grown at
1029 26°C or 37°C/low calcium.

1030

1031 **Figure S3. The *pil*::Tn strain exhibits normal temperature and calcium regulation of T3SS**
1032 **activity.** Strains were grown in regular LB or low calcium LB media, at either 26°C or at 37°C.
1033 Secreted proteins in the supernatant were precipitated and visualized by SDS-PAGE and
1034 Coomassie blue staining. Bovine serum albumin (BSA) was added as a loading and
1035 precipitation control. Data shown is representative data of three biological replicates.

1036

1037 **Figure S4. Transposon insertion in the *pil* locus alters RNA-Seq read patterns at the *cop-***
1038 ***rep* locus.** Reads from RNA-seq analysis mapped to the *cop-rep* locus and adjacent *pil* locus
1039 from wildtype and *pil*::Tn (*pil*) *Y. pseudotuberculosis* IP2666pIB1 grown at 26°C or 37°C/low
1040 calcium. The putative *pil* locus is indicated by a black box and the approximate location of the
1041 Tn insertion is indicated with an arrow.

1042

1043 **Figure S5. The *pcnB* gene is required for plasmid-mediated antibiotic resistance in**
1044 ***Y. pseudotuberculosis.*** Wildtype and Δ*pcnB Y. pseudotuberculosis* IP2666pIB1 harboring
1045 either pBAD33 or pACYC184 were grown overnight in LB supplemented with 20 µg/mL
1046 chloramphenicol, and the overnight cultures spotted onto LB agar lacking or containing
1047 chloramphenicol to assess plasmid retention. Plates were incubated at 26°C for ~16 hours
1048 before imaging. Each experiment was carried out for a total of two independent experiments.

1049

1050 **Figure S6. *Y. pseudotuberculosis* isolated from infected livers demonstrate similar**
1051 **plasmid loss and T3SS activity phenotypes as their parental strains.** Independent colony
1052 forming units from infected mouse livers were isolated and assessed for their ability to retain
1053 pYV and carry out T3SS activity. WT-3 and WT-5 are wildtype IP2666pIB1-derived isolates from
1054 two different mice. Δ*pcnB*-2-9, Δ*pcnB*-2-10, Δ*pcnB*-3-1, and Δ*pcnB*-3-2 are Δ*pcnB*-derived
1055 isolates from two different mice. **(A)** Liver isolates and their parental strains were incubated
1056 overnight at 26˚C in LB or 37˚C in LB/low calcium media. Colonies were patched onto low
1057 calcium media containing Congo red to induce T3SS activity and assess the percentage of
1058 colonies that retained pYV (i.e.-red colonies). **(B)** Liver isolates and their parental strains were
1059 incubated in LB low calcium media at 37˚C, and secreted proteins visualized by Coomassie blue
1060 staining. Bovine serum albumin (BSA) was added as a loading and precipitation control. Data
1061 shown is representative of two independent experiments.

1062

1063 **Figure S7. Loss of PAP I does not affect *Y. pseudotuberculosis* growth following stress**
1064 **exposure. (A)** Wildtype and Δ*pcnB Y. pseudotuberculosis* IP2666pIB1 cultures were grown to
1065 mid-log phase at 26°C before shifting to 42°C for 1 hour to induce heat shock. Spot dilutions
1066 were plated onto LB plates and incubated at 26°C for ~16 hours before imaging. **(B)** Strains in

1067 the IP2666pIB1 background were grown at 26°C overnight (stationary phase) before diluting
1068 and spotting into LB plates. Plates were incubated at 26°C for 4 hours before transferring to 4°C
1069 and allowing growth for ~2 days prior to imaging. **(C)** Wildtype and Δ*pcnB Y.*
1070 *pseudotuberculosis* IP2666pIB1 were grown at 37°C (low calcium) to mid-log phase before
1071 inducing stress. Growth was assayed by plating spot dilutions following stress exposure. Stress
1072 was induced by adjusting media to pH=3.0 to induce acid shock or by addition of 800Mm $NaCl_2$
1073 to induce osmotic shock.

1074

1075 **Figure S8. PAP I from *Y. pseudotuberculosis* and *Y. pestis* are 100% conserved.** Predicted
1076 PAP I sequences from *Y. pseudotuberculosis* IP2666pIB1 and *Y. pestis* KIM5.

1077

1078 **Figure S9. *Y. pseudotuberculosis* displays normal T3SS activity in EZ-RDM low calcium**
1079 **media.** *Y. pseudotuberculosis* IP2666pIB1 wildtype, Δ*pcnB*, and pYV- strains were grown in
1080 either low calcium LB or low calcium EZ-RDM media. The pYV- strain cured of pYV was used
1081 as a negative control [103]. Secreted proteins were visualized by Coomassie blue staining.
1082 Bovine serum albumin (BSA) was added as a loading and precipitation control. Data shown is
1083 representative of two independent experiments.

1084

1085 **Table S1. Phenotypic categories and mutations identified in suppressor screen.**

1086

1087 **Table S2. *Y. pseudotuberculosis* strains used in this study.**

1088

1089 **Table S3. Primers used in this study.**

1090

1091 **Table S4. Plasmids used in this study.**

1092

1093 **Dataset S1. Transcriptome analysis of *Y. pseudotuberculosis* IP2666pIB1, *pil*::Tn, Δ*pcnB*,**

1094 **and *pil*::Tn/Δ*pcnB* congenic strains.**

1095 **References**

1096 1. Pilla G, Tang CM. Going around in circles: virulence plasmids in enteric pathogens. Nat
1097 Rev Microbiol. 2018;16(8):484-95. doi: 10.1038/s41579-018-0031-2. PubMed PMID: 29855597.
1098 2. Gemski P, Lazere JR, Casey T, Wohlhieter JA. Presence of a virulence-associated
1099 plasmid in *Yersinia pseudotuberculosis*. Infect Immun. 1980;28(3):1044-7. doi:
1100 10.1128/iai.28.3.1044-1047.1980. PubMed PMID: 6249747; PubMed Central PMCID:
1101 PMCPMC551057.
1102 3. Cornelis GR. The *Yersinia* Yop virulon, a bacterial system to subvert cells of the primary
1103 host defense. Folia Microbiol (Praha). 1998;43(3):253-61. doi: 10.1007/BF02818610. PubMed
1104 PMID: 9717252.
1105 4. Sun YC, Jarrett CO, Bosio CF, Hinnebusch BJ. Retracing the evolutionary path that led
1106 to flea-borne transmission of *Yersinia pestis*. Cell Host Microbe. 2014;15(5):578-86. doi:
1107 10.1016/j.chom.2014.04.003. PubMed PMID: 24832452; PubMed Central PMCID:
1108 PMCPMC4084870.
1109 5. Glatter KA, Finkelman P. History of the Plague: An Ancient Pandemic for the Age of
1110 COVID-19. Am J Med. 2021;134(2):176-81. Epub 20200924. doi:
1111 10.1016/j.amjmed.2020.08.019. PubMed PMID: 32979306; PubMed Central PMCID:
1112 PMCPMC7513766.
1113 6. Cornelis GR, Boland A, Boyd AP, Geuijen C, Iriarte M, Neyt C, et al. The virulence
1114 plasmid of *Yersinia*, an antihost genome. Microbiol Mol Biol Rev. 1998;62(4):1315-52. doi:
1115 10.1128/MMBR.62.4.1315-1352.1998. PubMed PMID: 9841674; PubMed Central PMCID:
1116 PMCPMC98948.
1117 7. Portnoy DA, Wolf-Watz H, Bolin I, Beeder AB, Falkow S. Characterization of common
1118 virulence plasmids in *Yersinia* species and their role in the expression of outer membrane

1119 proteins. Infect Immun. 1984;43(1):108-14. doi: 10.1128/iai.43.1.108-114.1984. PubMed PMID:
1120 6317562; PubMed Central PMCID: PMCPMC263395.
1121 8. Demeure C, Dussurget O, Fiol GM, Le Guern AS, Savin C, Pizarro-Cerda J. *Yersinia*
1122 *pestis* and plague: an updated view on evolution, virulence determinants, immune subversion,
1123 vaccination and diagnostics. Microbes Infect. 2019;21(5-6):202-12. Epub 20190625. doi:
1124 10.1016/j.micinf.2019.06.007. PubMed PMID: 31252217.
1125 9. Cornelis GR. The type III secretion injectisome. Nat Rev Microbiol. 2006;4(11):811-25.
1126 doi: 10.1038/nrmicro1526. PubMed PMID: 17041629.
1127 10. Coburn B, Sekirov I, Finlay BB. Type III secretion systems and disease. Clin Microbiol
1128 Rev. 2007;20(4):535-49. doi: 10.1128/CMR.00013-07. PubMed PMID: 17934073; PubMed
1129 Central PMCID: PMCPMC2176049.
1130 11. Bliska JB, Wang X, Viboud GI, Brodsky IE. Modulation of innate immune responses by
1131 *Yersinia* type III secretion system translocators and effectors. Cell Microbiol. 2013;15(10):1622-
1132 31. Epub 20130729. doi: 10.1111/cmi.12164. PubMed PMID: 23834311; PubMed Central
1133 PMCID: PMCPMC3788085.
1134 12. Deng W, Marshall NC, Rowland JL, McCoy JM, Worrall LJ, Santos AS, et al. Assembly,
1135 structure, function and regulation of type III secretion systems. Nat Rev Microbiol.
1136 2017;15(6):323-37. Epub 20170410. doi: 10.1038/nrmicro.2017.20. PubMed PMID: 28392566.
1137 13. Schubert KA, Xu Y, Shao F, Auerbuch V. The *Yersinia* Type III Secretion System as a
1138 Tool for Studying Cytosolic Innate Immune Surveillance. Annu Rev Microbiol. 2020;74:221-45.
1139 Epub 20200713. doi: 10.1146/annurev-micro-020518-120221. PubMed PMID: 32660389.
1140 14. Brubaker RR. The Vwa+ virulence factor of yersiniae: the molecular basis of the
1141 attendant nutritional requirement for Ca++. Rev Infect Dis. 1983;5 Suppl 4:S748-58. doi:
1142 10.1093/clinids/5.supplement_4.s748. PubMed PMID: 6195719.
1143 15. Sturm A, Heinemann M, Arnoldini M, Benecke A, Ackermann M, Benz M, et al. The cost
1144 of virulence: retarded growth of *Salmonella* Typhimurium cells expressing type III secretion

1145 system 1. PLoS Pathog. 2011;7(7):e1002143. Epub 20110728. doi:
1146 10.1371/journal.ppat.1002143. PubMed PMID: 21829349; PubMed Central PMCID:
1147 PMCPMC3145796.
1148 16. Milne-Davies B, Helbig C, Wimmi S, Cheng DWC, Paczia N, Diepold A. Life After
1149 Secretion-*Yersinia enterocolitica* Rapidly Toggles Effector Secretion and Can Resume Cell
1150 Division in Response to Changing External Conditions. Front Microbiol. 2019;10:2128. Epub
1151 20190913. doi: 10.3389/fmicb.2019.02128. PubMed PMID: 31572334; PubMed Central PMCID:
1152 PMCPMC6753693.
1153 17. Bolin I, Portnoy DA, Wolf-Watz H. Expression of the temperature-inducible outer
1154 membrane proteins of yersiniae. Infect Immun. 1985;48(1):234-40. doi: 10.1128/iai.48.1.234-
1155 240.1985. PubMed PMID: 3980086; PubMed Central PMCID: PMCPMC261940.
1156 18. Bohme K, Steinmann R, Kortmann J, Seekircher S, Heroven AK, Berger E, et al.
1157 Concerted actions of a thermo-labile regulator and a unique intergenic RNA thermosensor
1158 control *Yersinia* virulence. PLoS Pathog. 2012;8(2):e1002518. Epub 20120216. doi:
1159 10.1371/journal.ppat.1002518. PubMed PMID: 22359501; PubMed Central PMCID:
1160 PMCPMC3280987.
1161 19. Dewoody RS, Merritt PM, Marketon MM. Regulation of the *Yersinia* type III secretion
1162 system: traffic control. Front Cell Infect Microbiol. 2013;3:4. Epub 20130206. doi:
1163 10.3389/fcimb.2013.00004. PubMed PMID: 23390616; PubMed Central PMCID:
1164 PMCPMC3565153.
1165 20. Hoe NP, Goguen JD. Temperature sensing in *Yersinia pestis*: translation of the LcrF
1166 activator protein is thermally regulated. J Bacteriol. 1993;175(24):7901-9. doi:
1167 10.1128/jb.175.24.7901-7909.1993. PubMed PMID: 7504666; PubMed Central PMCID:
1168 PMCPMC206968.
1169 21. Wang H, Avican K, Fahlgren A, Erttmann SF, Nuss AM, Dersch P, et al. Increased
1170 plasmid copy number is essential for *Yersinia* T3SS function and virulence. Science.

1171 2016;353(6298):492-5. Epub 20160630. doi: 10.1126/science.aaf7501. PubMed PMID:
1172 27365311.
1173 22. Schneiders S, Hechard T, Edgren T, Avican K, Fallman M, Fahlgren A, et al.
1174 Spatiotemporal Variations in Growth Rate and Virulence Plasmid Copy Number during *Yersinia*
1175 *pseudotuberculosis* Infection. Infect Immun. 2021;89(4). Epub 20210317. doi:
1176 10.1128/IAI.00710-20. PubMed PMID: 33495272; PubMed Central PMCID: PMCPMC8090943.
1177 23. Schott S, Scheuer R, Ermoli F, Glatter T, Evguenieva-Hackenberg E, Diepold A. A
1178 ParDE toxin-antitoxin system is responsible for the maintenance of the *Yersinia* virulence
1179 plasmid but not for type III secretion-associated growth inhibition. Front Cell Infect Microbiol.
1180 2023;13:1166077. Epub 20230509. doi: 10.3389/fcimb.2023.1166077. PubMed PMID:
1181 37228670; PubMed Central PMCID: PMCPMC10203498.
1182 24. Villa L, Garcia-Fernandez A, Fortini D, Carattoli A. Replicon sequence typing of IncF
1183 plasmids carrying virulence and resistance determinants. J Antimicrob Chemother.
1184 2010;65(12):2518-29. Epub 20101008. doi: 10.1093/jac/dkq347. PubMed PMID: 20935300.
1185 25. Nordstrom K. Plasmid R1--replication and its control. Plasmid. 2006;55(1):1-26. Epub
1186 20050930. doi: 10.1016/j.plasmid.2005.07.002. PubMed PMID: 16199086.
1187 26. Meynell E, Datta N. The relation of resistance transfer factors to the F-factor (sex-factor)
1188 of *Escherichia coli* K12. Genet Res. 1966;7(1):134-40. doi: 10.1017/s0016672300009538.
1189 PubMed PMID: 5324663.
1190 27. Datta N, Kontomichalou P. Penicillinase synthesis controlled by infectious R factors in
1191 Enterobacteriaceae. Nature. 1965;208(5007):239-41. doi: 10.1038/208239a0. PubMed PMID:
1192 5326330.
1193 28. Olsson JA, Paulsson J, Nordstrom K. Effect of the CopB auxiliary replication control
1194 system on stability of maintenance of Par(+) plasmid R1. J Bacteriol. 2004;186(1):207-11. doi:
1195 10.1128/JB.186.1.207-211.2004. PubMed PMID: 14679240; PubMed Central PMCID:
1196 PMCPMC303431.

1197 29. Lopilato J, Bortner S, Beckwith J. Mutations in a new chromosomal gene of *Escherichia*
1198 *coli* K-12, *pcnB*, reduce plasmid copy number of pBR322 and its derivatives. Mol Gen Genet.
1199 1986;205(2):285-90. doi: 10.1007/BF00430440. PubMed PMID: 3100913.
1200 30. Liu JD, Parkinson JS. Genetics and sequence analysis of the *pcnB* locus, an
1201 *Escherichia coli* gene involved in plasmid copy number control. J Bacteriol. 1989;171(3):1254-
1202 61. doi: 10.1128/jb.171.3.1254-1261.1989. PubMed PMID: 2537812; PubMed Central PMCID:
1203 PMCPMC209738.
1204 31. Sippel AE. Purification and characterization of adenosine triphosphate: ribonucleic acid
1205 adenyltransferase from *Escherichia coli*. Eur J Biochem. 1973;37(1):31-40. doi: 10.1111/j.1432-
1206 1033.1973.tb02953.x. PubMed PMID: 4580885.
1207 32. Cao GJ, Sarkar N. Identification of the gene for an *Escherichia coli* poly(A) polymerase.
1208 Proc Natl Acad Sci U S A. 1992;89(21):10380-4. doi: 10.1073/pnas.89.21.10380. PubMed
1209 PMID: 1438224; PubMed Central PMCID: PMCPMC50342.
1210 33. Martin G, Keller W. Mutational analysis of mammalian poly(A) polymerase identifies a
1211 region for primer binding and catalytic domain, homologous to the family X polymerases, and to
1212 other nucleotidyltransferases. EMBO J. 1996;15(10):2593-603. PubMed PMID: 8665867;
1213 PubMed Central PMCID: PMCPMC450192.
1214 34. Masters M, March JB, Oliver IR, Collins JF. A possible role for the *pcnB* gene product of
1215 *Escherichia coli* in modulating RNA: RNA interactions. Mol Gen Genet. 1990;220(2):341-4. doi:
1216 10.1007/BF00260507. PubMed PMID: 1691435.
1217 35. Yue D, Maizels N, Weiner AM. CCA-adding enzymes and poly(A) polymerases are all
1218 members of the same nucleotidyltransferase superfamily: characterization of the CCA-adding
1219 enzyme from the archaeal hyperthermophile *Sulfolobus shibatae*. RNA. 1996;2(9):895-908.
1220 PubMed PMID: 8809016; PubMed Central PMCID: PMCPMC1369424.

1221 36. Jones GH. Acquisition of pcnB [poly(A) polymerase I] genes via horizontal transfer from
1222 the beta, gamma-Proteobacteria. Microb Genom. 2021;7(2). doi: 10.1099/mgen.0.000508.
1223 PubMed PMID: 33502308; PubMed Central PMCID: PMCPMC8208693.
1224 37. Maes A, Gracia C, Innocenti N, Zhang K, Aurell E, Hajnsdorf E. Landscape of RNA
1225 polyadenylation in *E. coli*. Nucleic Acids Res. 2017;45(5):2746-56. doi: 10.1093/nar/gkw894.
1226 PubMed PMID: 28426097; PubMed Central PMCID: PMCPMC5389530.
1227 38. Joanny G, Le Derout J, Brechemier-Baey D, Labas V, Vinh J, Regnier P, et al.
1228 Polyadenylation of a functional mRNA controls gene expression in *Escherichia coli*. Nucleic
1229 Acids Res. 2007;35(8):2494-502. Epub 20070329. doi: 10.1093/nar/gkm120. PubMed PMID:
1230 17395638; PubMed Central PMCID: PMCPMC1885654.
1231 39. Reichenbach B, Maes A, Kalamorz F, Hajnsdorf E, Gorke B. The small RNA GlmY acts
1232 upstream of the sRNA GlmZ in the activation of glmS expression and is subject to regulation by
1233 polyadenylation in *Escherichia coli*. Nucleic Acids Res. 2008;36(8):2570-80. Epub 20080311.
1234 doi: 10.1093/nar/gkn091. PubMed PMID: 18334534; PubMed Central PMCID:
1235 PMCPMC2377431.
1236 40. Mohanty BK, Maples VF, Kushner SR. Polyadenylation helps regulate functional tRNA
1237 levels in *Escherichia coli*. Nucleic Acids Res. 2012;40(10):4589-603. Epub 20120128. doi:
1238 10.1093/nar/gks006. PubMed PMID: 22287637; PubMed Central PMCID: PMCPMC3378859.
1239 41. Holmqvist E, Wagner EGH. Impact of bacterial sRNAs in stress responses. Biochem
1240 Soc Trans. 2017;45(6):1203-12. Epub 20171103. doi: 10.1042/BST20160363. PubMed PMID:
1241 29101308; PubMed Central PMCID: PMCPMC5730939.
1242 42. Sinha D, Matz LM, Cameron TA, De Lay NR. Poly(A) polymerase is required for RyhB
1243 sRNA stability and function in *Escherichia coli*. RNA. 2018;24(11):1496-511. Epub 20180730.
1244 doi: 10.1261/rna.067181.118. PubMed PMID: 30061117; PubMed Central PMCID:
1245 PMCPMC6191717.

1246 43. Francis N, Laishram RS. Transgenesis of mammalian PABP reveals mRNA
1247 polyadenylation as a general stress response mechanism in bacteria. iScience.
1248 2021;24(10):103119. Epub 20210911. doi: 10.1016/j.isci.2021.103119. PubMed PMID:
1249 34646982; PubMed Central PMCID: PMCPMC8496165.
1250 44. Masters M, Colloms MD, Oliver IR, He L, Macnaughton EJ, Charters Y. The *pcnB* gene
1251 of *Escherichia coli*, which is required for ColE1 copy number maintenance, is dispensable. J
1252 Bacteriol. 1993;175(14):4405-13. doi: 10.1128/jb.175.14.4405-4413.1993. PubMed PMID:
1253 8331071; PubMed Central PMCID: PMCPMC204881.
1254 45. Xu F, Lin-Chao S, Cohen SN. The *Escherichia coli pcnB* gene promotes adenylylation of
1255 antisense RNAI of ColE1-type plasmids in vivo and degradation of RNAI decay intermediates.
1256 Proc Natl Acad Sci U S A. 1993;90(14):6756-60. doi: 10.1073/pnas.90.14.6756. PubMed PMID:
1257 7688127; PubMed Central PMCID: PMCPMC47011.
1258 46. He L, Soderbom F, Wagner EG, Binnie U, Binns N, Masters M. PcnB is required for the
1259 rapid degradation of RNAI, the antisense RNA that controls the copy number of ColE1-related
1260 plasmids. Mol Microbiol. 1993;9(6):1131-42. doi: 10.1111/j.1365-2958.1993.tb01243.x. PubMed
1261 PMID: 7523833.
1262 47. Soderbom F, Binnie U, Masters M, Wagner EG. Regulation of plasmid R1 replication:
1263 PcnB and RNase E expedite the decay of the antisense RNA, CopA. Mol Microbiol.
1264 1997;26(3):493-504. doi: 10.1046/j.1365-2958.1997.5871953.x. PubMed PMID: 9402020.
1265 48. Pienkoss S, Javadi S, Chaoprasid P, Holler M, Rossmanith J, Dersch P, et al. RNA
1266 Thermometer-coordinated Assembly of the *Yersinia* Injectisome. J Mol Biol.
1267 2022;434(18):167667. Epub 20220603. doi: 10.1016/j.jmb.2022.167667. PubMed PMID:
1268 35667470.
1269 49. Kupferberg LL, Higuchi K. Role of calcium ions in the stimulation of growth of virulent
1270 strains of *Pasteurella pestis*. J Bacteriol. 1958;76(1):120-1. doi: 10.1128/jb.76.1.120-121.1958.
1271 PubMed PMID: 13563403; PubMed Central PMCID: PMCPMC290166.

1272 50. Higuchi K, Kupferberg LL, Smith JL. Studies on the nutrition and physiology of
1273 *Pasteurella pestis*. III. Effects of calcium ions on the growth of virulent and avirulent strains of
1274 *Pasteurella pestis*. J Bacteriol. 1959;77(3):317-21. doi: 10.1128/jb.77.3.317-321.1959. PubMed
1275 PMID: 13641190; PubMed Central PMCID: PMCPMC290369.
1276 51. Rosqvist R, Magnusson KE, Wolf-Watz H. Target cell contact triggers expression and
1277 polarized transfer of *Yersinia* YopE cytotoxin into mammalian cells. EMBO J. 1994;13(4):964-
1278 72. doi: 10.1002/j.1460-2075.1994.tb06341.x. PubMed PMID: 8112310; PubMed Central
1279 PMCID: PMCPMC394898.
1280 52. Takacs CN, Wachter J, Xiang Y, Ren Z, Karaboja X, Scott M, et al. Polyploidy, regular
1281 patterning of genome copies, and unusual control of DNA partitioning in the Lyme disease
1282 spirochete. Nat Commun. 2022;13(1):7173. Epub 20221122. doi: 10.1038/s41467-022-34876-4.
1283 PubMed PMID: 36450725; PubMed Central PMCID: PMCPMC9712426.
1284 53. Erdmann N, Petroff T, Funnell BE. Intracellular localization of P1 ParB protein depends
1285 on ParA and parS. Proc Natl Acad Sci U S A. 1999;96(26):14905-10. doi:
1286 10.1073/pnas.96.26.14905. PubMed PMID: 10611311; PubMed Central PMCID:
1287 PMCPMC24746.
1288 54. Wang JD, Levin PA. Metabolism, cell growth and the bacterial cell cycle. Nat Rev
1289 Microbiol. 2009;7(11):822-7. Epub 20091006. doi: 10.1038/nrmicro2202. PubMed PMID:
1290 19806155; PubMed Central PMCID: PMCPMC2887316.
1291 55. Cooper S, Helmstetter CE. Chromosome replication and the division cycle of
1292 *Escherichia coli* B/r. J Mol Biol. 1968;31(3):519-40. doi: 10.1016/0022-2836(68)90425-7.
1293 PubMed PMID: 4866337.
1294 56. Miller HK, Kwuan L, Schwiesow L, Bernick DL, Mettert E, Ramirez HA, et al. IscR is
1295 essential for *Yersinia pseudotuberculosis* type III secretion and virulence. PLoS Pathog.
1296 2014;10(6):e1004194. Epub 20140612. doi: 10.1371/journal.ppat.1004194. PubMed PMID:
1297 24945271; PubMed Central PMCID: PMCPMC4055776.

1298 57. Zhou P, She Y, Dong N, Li P, He H, Borio A, et al. Alpha-kinase 1 is a cytosolic innate
1299 immune receptor for bacterial ADP-heptose. Nature. 2018;561(7721):122-6. Epub 20180815.
1300 doi: 10.1038/s41586-018-0433-3. PubMed PMID: 30111836.
1301 58. Orth K, Palmer LE, Bao ZQ, Stewart S, Rudolph AE, Bliska JB, et al. Inhibition of the
1302 mitogen-activated protein kinase kinase superfamily by a *Yersinia* effector. Science.
1303 1999;285(5435):1920-3. doi: 10.1126/science.285.5435.1920. PubMed PMID: 10489373.
1304 59. Orth K, Xu Z, Mudgett MB, Bao ZQ, Palmer LE, Bliska JB, et al. Disruption of signaling
1305 by *Yersinia* effector YopJ, a ubiquitin-like protein protease. Science. 2000;290(5496):1594-7.
1306 doi: 10.1126/science.290.5496.1594. PubMed PMID: 11090361.
1307 60. Riley G, Toma S. Detection of pathogenic *Yersinia enterocolitica* by using congo red-
1308 magnesium oxalate agar medium. J Clin Microbiol. 1989;27(1):213-4. doi:
1309 10.1128/jcm.27.1.213-214.1989. PubMed PMID: 2913030; PubMed Central PMCID:
1310 PMCPMC267269.
1311 61. Raynal LC, Carpousis AJ. Poly(A) polymerase I of *Escherichia coli*: characterization of
1312 the catalytic domain, an RNA binding site and regions for the interaction with proteins involved
1313 in mRNA degradation. Mol Microbiol. 1999;32(4):765-75. doi: 10.1046/j.1365-
1314 2958.1999.01394.x. PubMed PMID: 10361280.
1315 62. Toh Y, Takeshita D, Nagaike T, Numata T, Tomita K. Mechanism for the alteration of the
1316 substrate specificities of template-independent RNA polymerases. Structure. 2011;19(2):232-
1317 43. doi: 10.1016/j.str.2010.12.006. PubMed PMID: 21300291.
1318 63. Million-Weaver S, Alexander DL, Allen JM, Camps M. Quantifying plasmid copy number
1319 to investigate plasmid dosage effects associated with directed protein evolution. Methods Mol
1320 Biol. 2012;834:33-48. doi: 10.1007/978-1-61779-483-4_3. PubMed PMID: 22144351; PubMed
1321 Central PMCID: PMCPMC3804865.

1322 64. Amann E, Ochs B, Abel KJ. Tightly regulated tac promoter vectors useful for the
1323 expression of unfused and fused proteins in *Escherichia coli.* Gene. 1988;69(2):301-15. doi:
1324 10.1016/0378-1119(88)90440-4. PubMed PMID: 3069586.
1325 65. Lacatena RM, Cesareni G. Base pairing of RNA I with its complementary sequence in
1326 the primer precursor inhibits ColE1 replication. Nature. 1981;294(5842):623-6. doi:
1327 10.1038/294623a0. PubMed PMID: 6171736.
1328 66. Brantl S. Plasmid Replication Control by Antisense RNAs. Microbiol Spectr.
1329 2014;2(4):PLAS-0001-2013. doi: 10.1128/microbiolspec.PLAS-0001-2013. PubMed PMID:
1330 26104196.
1331 67. Selzer G, Som T, Itoh T, Tomizawa J. The origin of replication of plasmid p15A and
1332 comparative studies on the nucleotide sequences around the origin of related plasmids. Cell.
1333 1983;32(1):119-29. doi: 10.1016/0092-8674(83)90502-0. PubMed PMID: 6186390.
1334 68. Uga H, Matsunaga F, Wada C. Regulation of DNA replication by iterons: an interaction
1335 between the ori2 and incC regions mediated by RepE-bound iterons inhibits DNA replication of
1336 mini-F plasmid in *Escherichia* coli. EMBO J. 1999;18(13):3856-67. doi:
1337 10.1093/emboj/18.13.3856. PubMed PMID: 10393200; PubMed Central PMCID:
1338 PMCPMC1171462.
1339 69. Jurenas D, Fraikin N, Goormaghtigh F, De Bruyn P, Vandervelde A, Zedek S, et al.
1340 Bistable Expression of a Toxin-Antitoxin System Located in a Cryptic Prophage of *Escherichia*
1341 *coli* O157:H7. mBio. 2021;12(6):e0294721. Epub 20211130. doi: 10.1128/mBio.02947-21.
1342 PubMed PMID: 34844426; PubMed Central PMCID: PMCPMC8630535.
1343 70. Mecsas J, Bilis I, Falkow S. Identification of attenuated *Yersinia pseudotuberculosis*
1344 strains and characterization of an orogastric infection in BALB/c mice on day 5 postinfection by
1345 signature-tagged mutagenesis. Infect Immun. 2001;69(5):2779-87. doi: 10.1128/IAI.67.5.2779-
1346 2787.2001. PubMed PMID: 11292689; PubMed Central PMCID: PMCPMC98225.

1347 71. Spickler C, Mackie GA. Action of RNase II and polynucleotide phosphorylase against
1348 RNAs containing stem-loops of defined structure. J Bacteriol. 2000;182(9):2422-7. doi:
1349 10.1128/JB.182.9.2422-2427.2000. PubMed PMID: 10762241; PubMed Central PMCID:
1350 PMCPMC111303.
1351 72. O'Hara EB, Chekanova JA, Ingle CA, Kushner ZR, Peters E, Kushner SR.
1352 Polyadenylylation helps regulate mRNA decay in *Escherichia coli*. Proc Natl Acad Sci U S A.
1353 1995;92(6):1807-11. doi: 10.1073/pnas.92.6.1807. PubMed PMID: 7534403; PubMed Central
1354 PMCID: PMCPMC42371.
1355 73. Hajnsdorf E, Braun F, Haugel-Nielsen J, Regnier P. Polyadenylylation destabilizes the
1356 rpsO mRNA of *Escherichia coli*. Proc Natl Acad Sci U S A. 1995;92(9):3973-7. doi:
1357 10.1073/pnas.92.9.3973. PubMed PMID: 7732015; PubMed Central PMCID: PMCPMC42084.
1358 74. Xu F, Cohen SN. RNA degradation in *Escherichia coli* regulated by 3' adenylation and 5'
1359 phosphorylation. Nature. 1995;374(6518):180-3. doi: 10.1038/374180a0. PubMed PMID:
1360 7533264.
1361 75. Blum E, Carpousis AJ, Higgins CF. Polyadenylation promotes degradation of 3'-
1362 structured RNA by the *Escherichia coli* mRNA degradosome in vitro. J Biol Chem.
1363 1999;274(7):4009-16. doi: 10.1074/jbc.274.7.4009. PubMed PMID: 9933592.
1364 76. Coburn GA, Miao X, Briant DJ, Mackie GA. Reconstitution of a minimal RNA
1365 degradosome demonstrates functional coordination between a 3' exonuclease and a DEAD-box
1366 RNA helicase. Genes Dev. 1999;13(19):2594-603. doi: 10.1101/gad.13.19.2594. PubMed
1367 PMID: 10521403; PubMed Central PMCID: PMCPMC317069.
1368 77. Marujo PE, Hajnsdorf E, Le Derout J, Andrade R, Arraiano CM, Regnier P. RNase II
1369 removes the oligo(A) tails that destabilize the rpsO mRNA of *Escherichia coli*. RNA.
1370 2000;6(8):1185-93. doi: 10.1017/s135583820000073x. PubMed PMID: 10943897; PubMed
1371 Central PMCID: PMCPMC1369992.

1372 78. Rosenzweig JA, Chromy B, Echeverry A, Yang J, Adkins B, Plano GV, et al.
1373 Polynucleotide phosphorylase independently controls virulence factor expression levels and
1374 export in *Yersinia* spp. FEMS Microbiol Lett. 2007;270(2):255-64. Epub 20070328. doi:
1375 10.1111/j.1574-6968.2007.00689.x. PubMed PMID: 17391372.
1376 79. Rosenzweig JA, Weltman G, Plano GV, Schesser K. Modulation of *Yersinia* type three
1377 secretion system by the S1 domain of polynucleotide phosphorylase. J Biol Chem.
1378 2005;280(1):156-63. Epub 20041026. doi: 10.1074/jbc.M405662200. PubMed PMID: 15509583.
1379 80. Knittel V, Vollmer I, Volk M, Dersch P. Discovering RNA-Based Regulatory Systems for
1380 *Yersinia* Virulence. Front Cell Infect Microbiol. 2018;8:378. Epub 20181025. doi:
1381 10.3389/fcimb.2018.00378. PubMed PMID: 30460205; PubMed Central PMCID:
1382 PMCPMC6232918.
1383 81. Mohanty BK, Maples VF, Kushner SR. The Sm-like protein Hfq regulates
1384 polyadenylation dependent mRNA decay in Escherichia coli. Mol Microbiol. 2004;54(4):905-20.
1385 doi: 10.1111/j.1365-2958.2004.04337.x. PubMed PMID: 15522076.
1386 82. Werbowy O, Boratynski R, Dekowska A, Kaczorowski T. Genetic analysis of
1387 maintenance of pEC156, a naturally occurring *Escherichia coli* plasmid that carries genes of the
1388 EcoVIII restriction-modification system. Plasmid. 2015;77:39-50. Epub 20141208. doi:
1389 10.1016/j.plasmid.2014.12.002. PubMed PMID: 25500017.
1390 83. Francis N, Behera MR, Natarajan K, Laishram RS. Tyrosine phosphorylation controlled
1391 poly(A) polymerase I activity regulates general stress response in bacteria. Life Sci Alliance.
1392 2023;6(3). Epub 20221219. doi: 10.26508/lsa.202101148. PubMed PMID: 36535710; PubMed
1393 Central PMCID: PMCPMC9764084.
1394 84. Ottoz DSM, Berchowitz LE. The role of disorder in RNA binding affinity and specificity.
1395 Open Biol. 2020;10(12):200328. Epub 20201223. doi: 10.1098/rsob.200328. PubMed PMID:
1396 33352065; PubMed Central PMCID: PMCPMC7776568.

1397 85. Milton DL, Norqvist A, Wolf-Watz H. Cloning of a metalloprotease gene involved in the
1398 virulence mechanism of *Vibrio anguillarum*. J Bacteriol. 1992;174(22):7235-44. doi:
1399 10.1128/jb.174.22.7235-7244.1992. PubMed PMID: 1429449; PubMed Central PMCID:
1400 PMCPMC207417.
1401 86. Bolger AM, Lohse M, Usadel B. Trimmomatic: a flexible trimmer for Illumina sequence
1402 data. Bioinformatics. 2014;30(15):2114-20. Epub 20140401. doi: 10.1093/bioinformatics/btu170.
1403 PubMed PMID: 24695404; PubMed Central PMCID: PMCPMC4103590.
1404 87. Li H, Durbin R. Fast and accurate short read alignment with Burrows-Wheeler transform.
1405 Bioinformatics. 2009;25(14):1754-60. Epub 20090518. doi: 10.1093/bioinformatics/btp324.
1406 PubMed PMID: 19451168; PubMed Central PMCID: PMCPMC2705234.
1407 88. Johnson SL, Daligault HE, Davenport KW, Jaissle J, Frey KG, Ladner JT, et al. Thirty-
1408 Two Complete Genome Assemblies of Nine *Yersinia* Species, Including *Y. pestis*, *Y.*
1409 *pseudotuberculosis*, and *Y. enterocolitica*. Genome Announc. 2015;3(2). Epub 20150430. doi:
1410 10.1128/genomeA.00148-15. PubMed PMID: 25931590; PubMed Central PMCID:
1411 PMCPMC4417686.
1412 89. Zoubeidi A, Schwiesow L, Auerbuch V, Lam HN. Complete Genome Assembly of
1413 *Yersinia pseudotuberculosis* IP2666pIB1. Microbiol Resour Announc. 2019;8(7). Epub
1414 20190214. doi: 10.1128/MRA.01592-18. PubMed PMID: 30801065; PubMed Central PMCID:
1415 PMCPMC6376424.
1416 90. Li H, Handsaker B, Wysoker A, Fennell T, Ruan J, Homer N, et al. The Sequence
1417 Alignment/Map format and SAMtools. Bioinformatics. 2009;25(16):2078-9. Epub 20090608. doi:
1418 10.1093/bioinformatics/btp352. PubMed PMID: 19505943; PubMed Central PMCID:
1419 PMCPMC2723002.
1420 91. Auwera Gvd, O'Connor BD. Genomics in the cloud : using Docker, GATK, and WDL in
1421 Terra. First edition. ed. Sebastopol, CA: O'Reilly Media; 2020. xxiv, 467 pages p.

1422 92. Hechard T, Wang H. Determination of Growth Rate and Virulence Plasmid Copy
1423 Number During *Yersinia pseudotuberculosis* Infection Using Droplet Digital PCR. Methods Mol
1424 Biol. 2023;2674:101-15. doi: 10.1007/978-1-0716-3243-7_7. PubMed PMID: 37258963.
1425 93. Paintdakhi A, Parry B, Campos M, Irnov I, Elf J, Surovtsev I, et al. Oufti: an integrated
1426 software package for high-accuracy, high-throughput quantitative microscopy analysis. Mol
1427 Microbiol. 2016;99(4):767-77. Epub 20151218. doi: 10.1111/mmi.13264. PubMed PMID:
1428 26538279; PubMed Central PMCID: PMCPMC4752901.
1429 94. Campos M, Govers SK, Irnov I, Dobihal GS, Cornet F, Jacobs-Wagner C. Genomewide
1430 phenotypic analysis of growth, cell morphogenesis, and cell cycle events in *Escherichia coli*. Mol
1431 Syst Biol. 2018;14(6):e7573. Epub 20180625. doi: 10.15252/msb.20177573. PubMed PMID:
1432 29941428; PubMed Central PMCID: PMCPMC6018989.
1433 95. Schindelin J, Arganda-Carreras I, Frise E, Kaynig V, Longair M, Pietzsch T, et al. Fiji: an
1434 open-source platform for biological-image analysis. Nat Methods. 2012;9(7):676-82. Epub
1435 20120628. doi: 10.1038/nmeth.2019. PubMed PMID: 22743772; PubMed Central PMCID:
1436 PMCPMC3855844.
1437 96. Ovesny M, Krizek P, Borkovec J, Svindrych Z, Hagen GM. ThunderSTORM: a
1438 comprehensive ImageJ plug-in for PALM and STORM data analysis and super-resolution
1439 imaging. Bioinformatics. 2014;30(16):2389-90. Epub 20140425. doi:
1440 10.1093/bioinformatics/btu202. PubMed PMID: 24771516; PubMed Central PMCID:
1441 PMCPMC4207427.
1442 97. Otsu N. A Threshold Selection Method from Gray-Level Histograms. IEEE Trans Syst
1443 Man Cybern. 1979;9(1):62-6.
1444 98. Kwuan L, Adams W, Auerbuch V. Impact of host membrane pore formation by the
1445 *Yersinia pseudotuberculosis* type III secretion system on the macrophage innate immune
1446 response. Infect Immun. 2013;81(3):905-14. Epub 20130107. doi: 10.1128/IAI.01014-12.
1447 PubMed PMID: 23297383; PubMed Central PMCID: PMCPMC3584892.

1448 99. Kim D, Paggi JM, Park C, Bennett C, Salzberg SL. Graph-based genome alignment and
1449 genotyping with HISAT2 and HISAT-genotype. Nat Biotechnol. 2019;37(8):907-15. Epub
1450 20190802. doi: 10.1038/s41587-019-0201-4. PubMed PMID: 31375807; PubMed Central
1451 PMCID: PMCPMC7605509.
1452 100. Liao Y, Smyth GK, Shi W. featureCounts: an efficient general purpose program for
1453 assigning sequence reads to genomic features. Bioinformatics. 2014;30(7):923-30. Epub
1454 20131113. doi: 10.1093/bioinformatics/btt656. PubMed PMID: 24227677.
1455 101. Robinson MD, McCarthy DJ, Smyth GK. edgeR: a Bioconductor package for differential
1456 expression analysis of digital gene expression data. Bioinformatics. 2010;26(1):139-40. Epub
1457 20091111. doi: 10.1093/bioinformatics/btp616. PubMed PMID: 19910308; PubMed Central
1458 PMCID: PMCPMC2796818.
1459 102. Metsalu T, Vilo J. ClustVis: a web tool for visualizing clustering of multivariate data using
1460 Principal Component Analysis and heatmap. Nucleic Acids Res. 2015;43(W1):W566-70. Epub
1461 20150512. doi: 10.1093/nar/gkv468. PubMed PMID: 25969447; PubMed Central PMCID:
1462 PMCPMC4489295.
1463 103. Auerbuch V, Golenbock DT, Isberg RR. Innate immune recognition of *Yersinia*
1464 *pseudotuberculosis* type III secretion. PLoS Pathog. 2009;5(12):e1000686. Epub 20091204.
1465 doi: 10.1371/journal.ppat.1000686. PubMed PMID: 19997504; PubMed Central PMCID:
1466 PMCPMC2779593.

1467

Figure 1

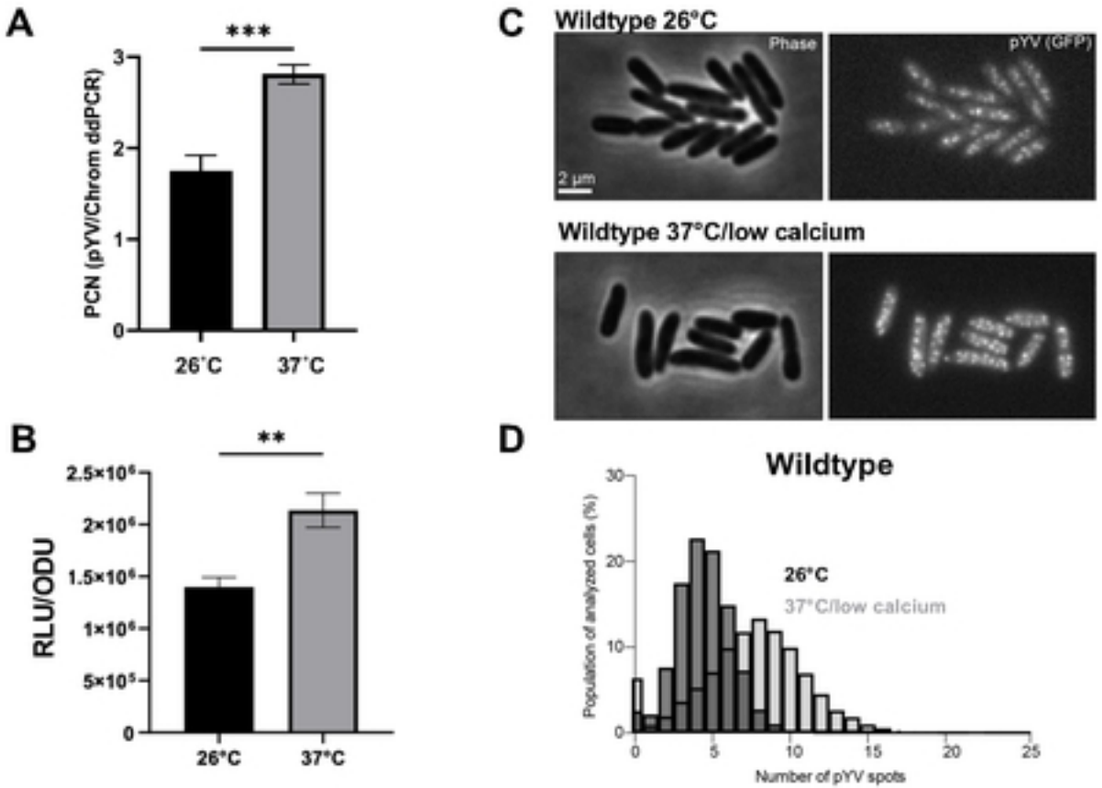
A
***
PCN (pYV/Chrom ddPCR)
3
2
1
0
26˚C
37˚C
B
**
RLU/ODU
2.5×10⁶
2×10⁶
1.5×10⁶
1×10⁶
5×10⁵
0
26°C
37°C
C
Wildtype 26°C
Phase
pYV (GFP)
2 µm
Wildtype 37°C/low calcium
D
Wildtype
Population of analyzed cells (%)
30
20
10
0
26°C
37°C/low calcium
0
5
10
15
20
25
Number of pYV spots

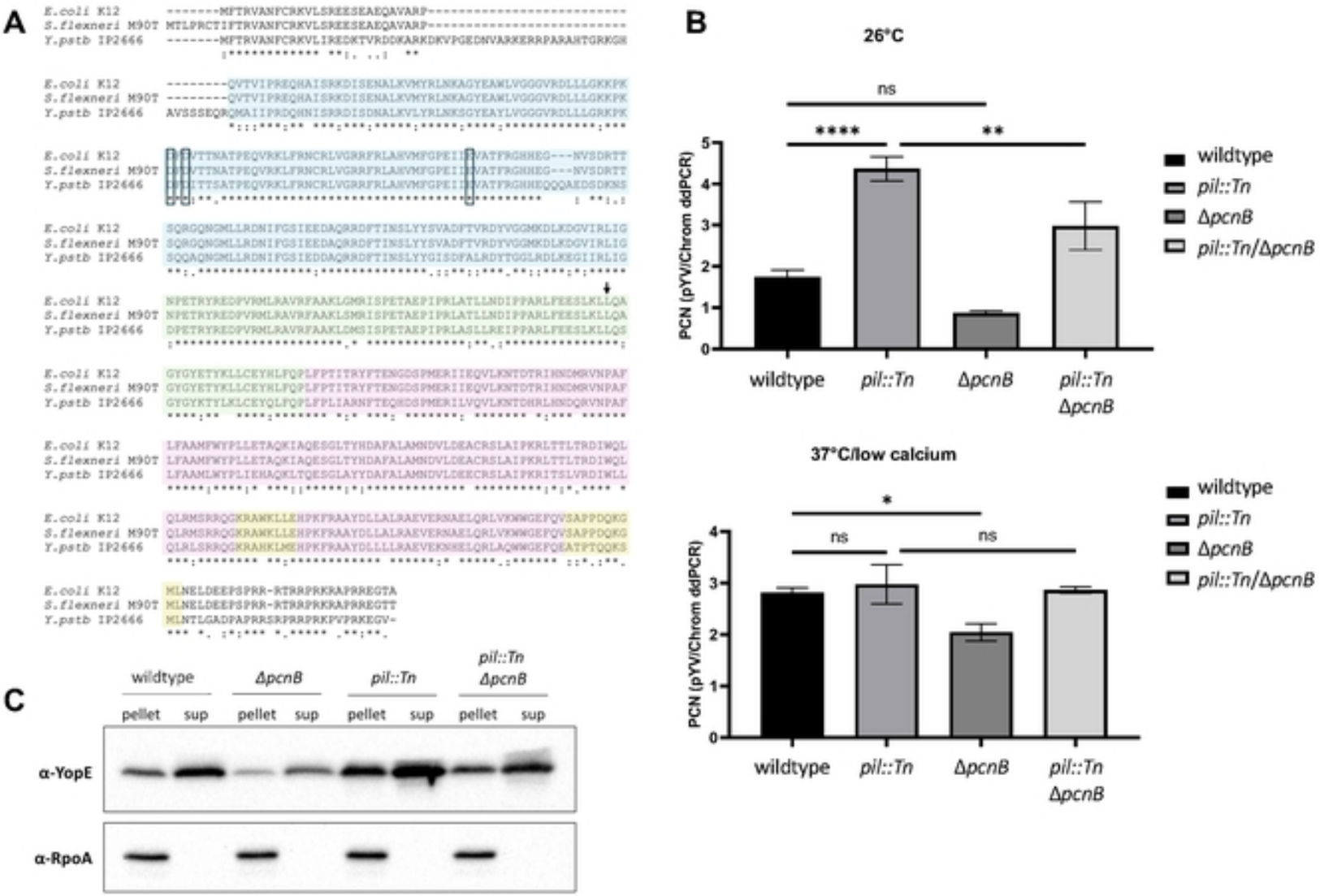
A
E.coli K12
S.flexneri M90T
Y.pstb IP2666
B
26°C
ns
****
**
PCN (pYV/Chrom ddPCR)
wildtype
pil::Tn
ΔpcnB
pil::Tn/ΔpcnB
37°C/low calcium
*
ns
ns
C
wildtype
ΔpcnB
pil::Tn
pil::Tn ΔpcnB
pellet
sup
α-YopE
α-RpoA

Figure 2

Figure 3

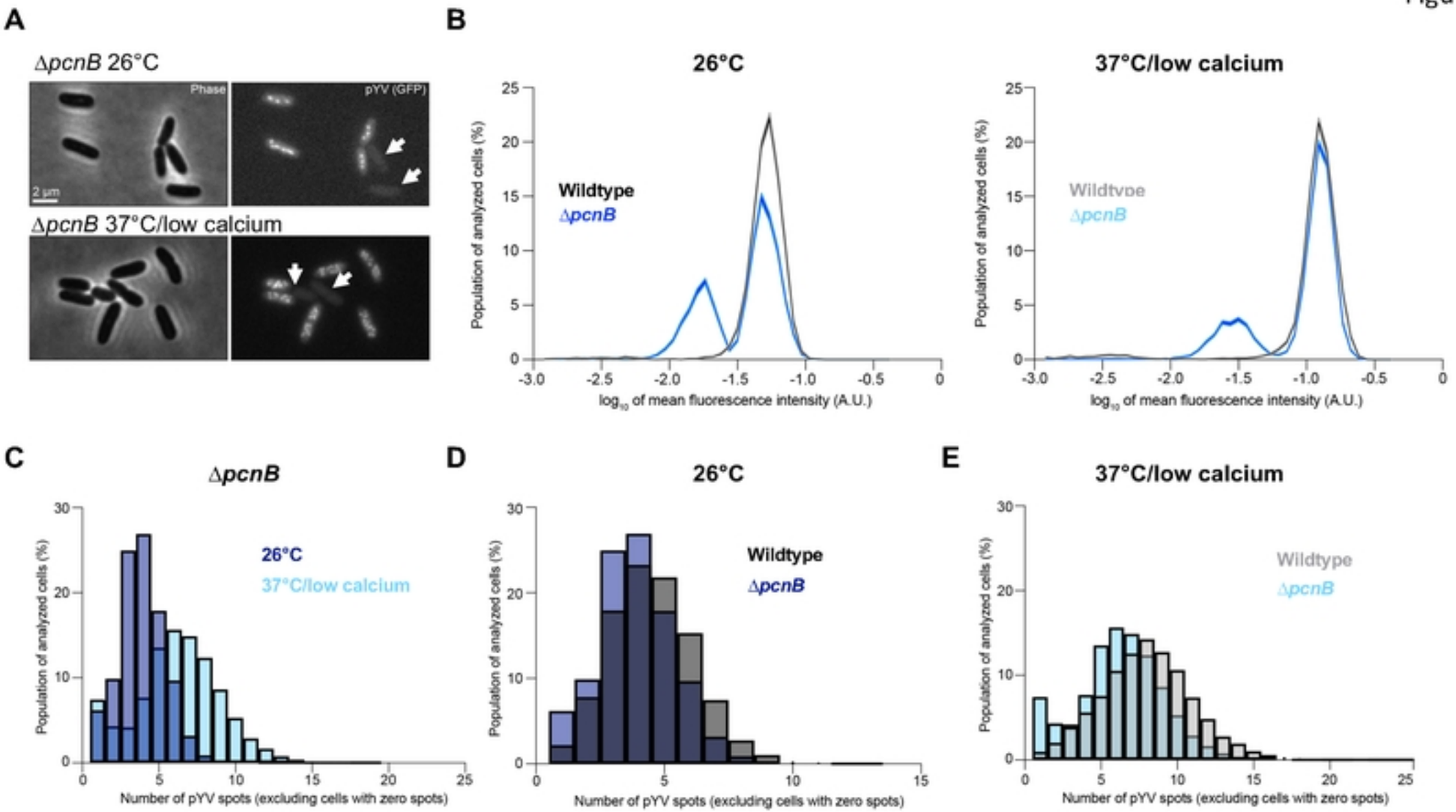
A
ΔpcnB 26°C
Phase
pYV (GFP)
2 µm
ΔpcnB 37°C/low calcium
B
26°C
Wildtype
ΔpcnB
Population of analyzed cells (%)
log10 of mean fluorescence intensity (A.U.)
37°C/low calcium
Wildtype
ΔpcnB
Population of analyzed cells (%)
log10 of mean fluorescence intensity (A.U.)
C
ΔpcnB
26°C
37°C/low calcium
Population of analyzed cells (%)
Number of pYV spots (excluding cells with zero spots)
D
26°C
Wildtype
ΔpcnB
Population of analyzed cells (%)
Number of pYV spots (excluding cells with zero spots)
E
37°C/low calcium
Wildtype
ΔpcnB
Population of analyzed cells (%)
Number of pYV spots (excluding cells with zero spots)

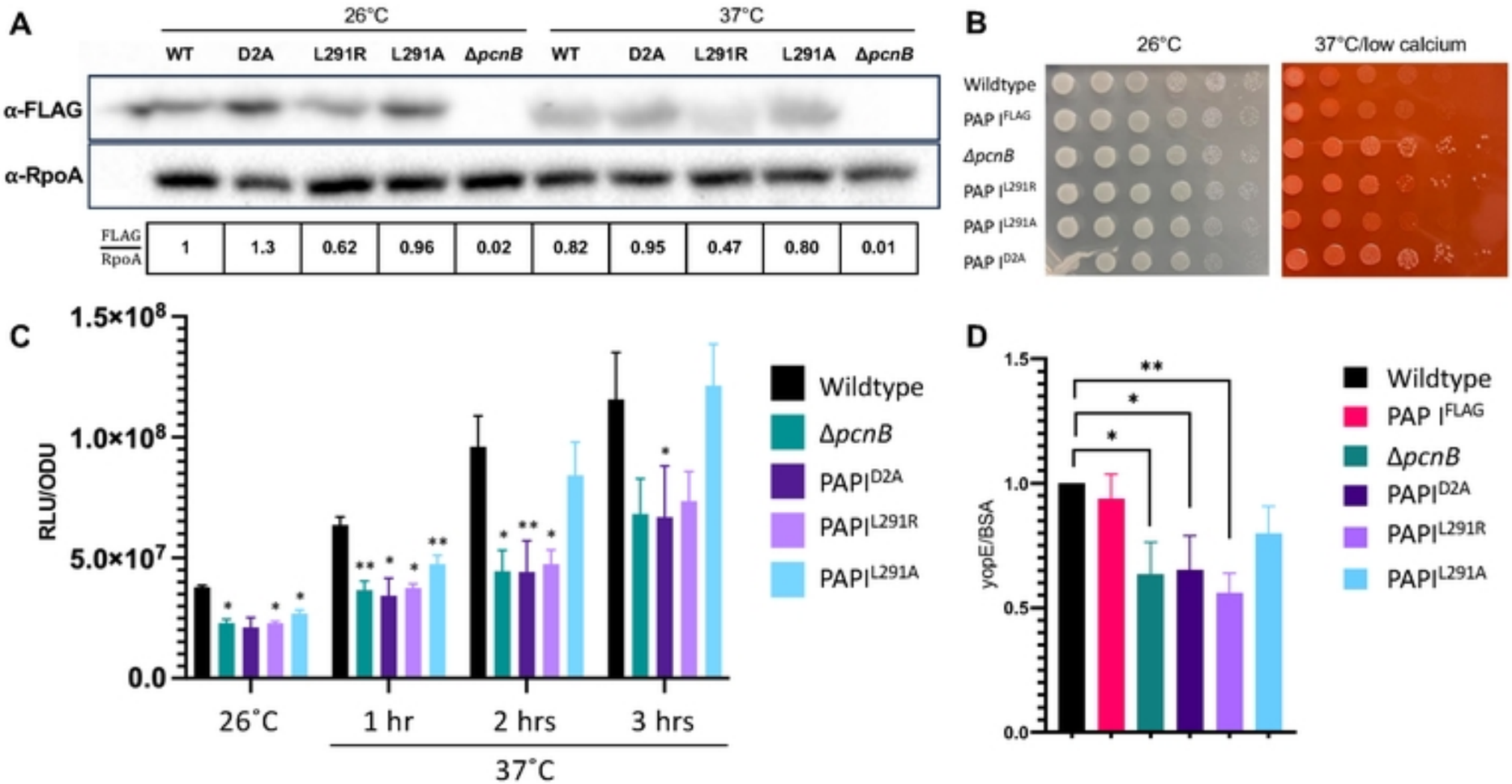
A
26°C
37°C
WT
D2A
L291R
L291A
ΔpcnB
WT
D2A
L291R
L291A
ΔpcnB
α-FLAG
α-RpoA
FLAG/RpoA
1
1.3
0.62
0.96
0.02
0.82
0.95
0.47
0.80
0.01
B
26°C
37°C/low calcium
Wildtype
PAP I^FLAG
ΔpcnB
PAP I^L291R
PAP I^L291A
PAP I^D2A
C
RLU/ODU
1.5×10^8
1.0×10^8
5.0×10^7
0.0
26˚C
1 hr
2 hrs
3 hrs
37˚C
Wildtype
ΔpcnB
PAPI^D2A
PAPI^L291R
PAPI^L291A
D
yopE/BSA
1.5
1.0
0.5
0.0
Wildtype
PAP I^FLAG
ΔpcnB
PAPI^D2A
PAPI^L291R
PAPI^L291A

Figure 4

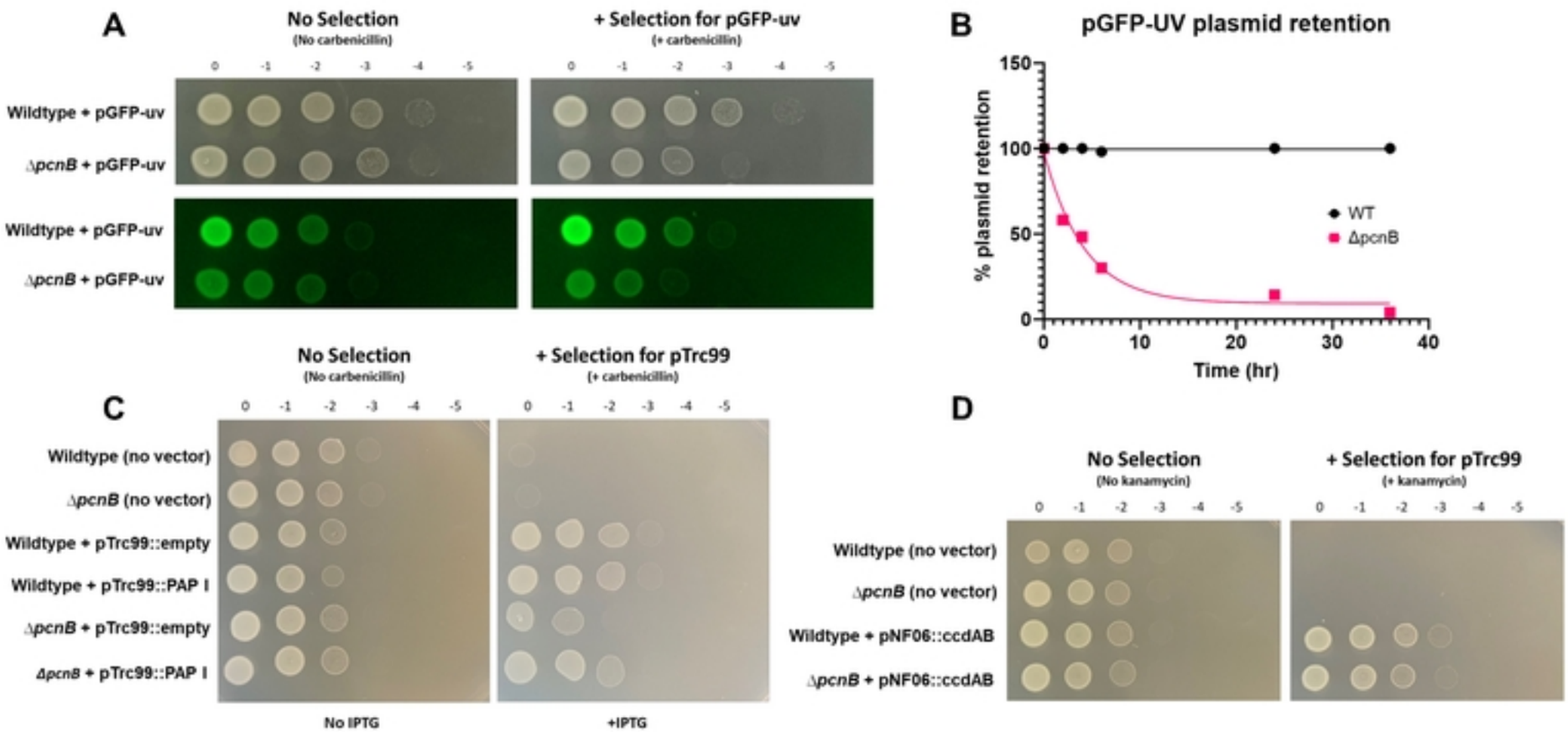
A
No Selection
(No carbenicillin)
+ Selection for pGFP-uv
(+ carbenicillin)
0 -1 -2 -3 -4 -5
Wildtype + pGFP-uv
ΔpcnB + pGFP-uv
Wildtype + pGFP-uv
ΔpcnB + pGFP-uv
B
pGFP-UV plasmid retention
% plasmid retention
150
100
50
0
0 10 20 30 40
Time (hr)
WT
ΔpcnB
C
No Selection
(No carbenicillin)
+ Selection for pTrc99
(+ carbenicillin)
0 -1 -2 -3 -4 -5
Wildtype (no vector)
ΔpcnB (no vector)
Wildtype + pTrc99::empty
Wildtype + pTrc99::PAP I
ΔpcnB + pTrc99::empty
ΔpcnB + pTrc99::PAP I
No IPTG
+IPTG
D
No Selection
(No kanamycin)
+ Selection for pTrc99
(+ kanamycin)
0 -1 -2 -3 -4 -5
Wildtype (no vector)
ΔpcnB (no vector)
Wildtype + pNF06::ccdAB
ΔpcnB + pNF06::ccdAB

Figure 5

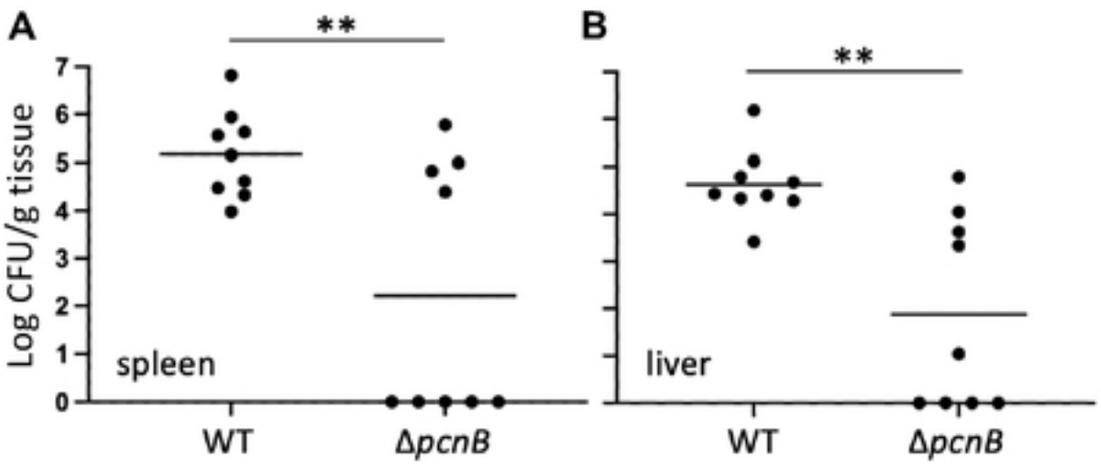

Figure 6

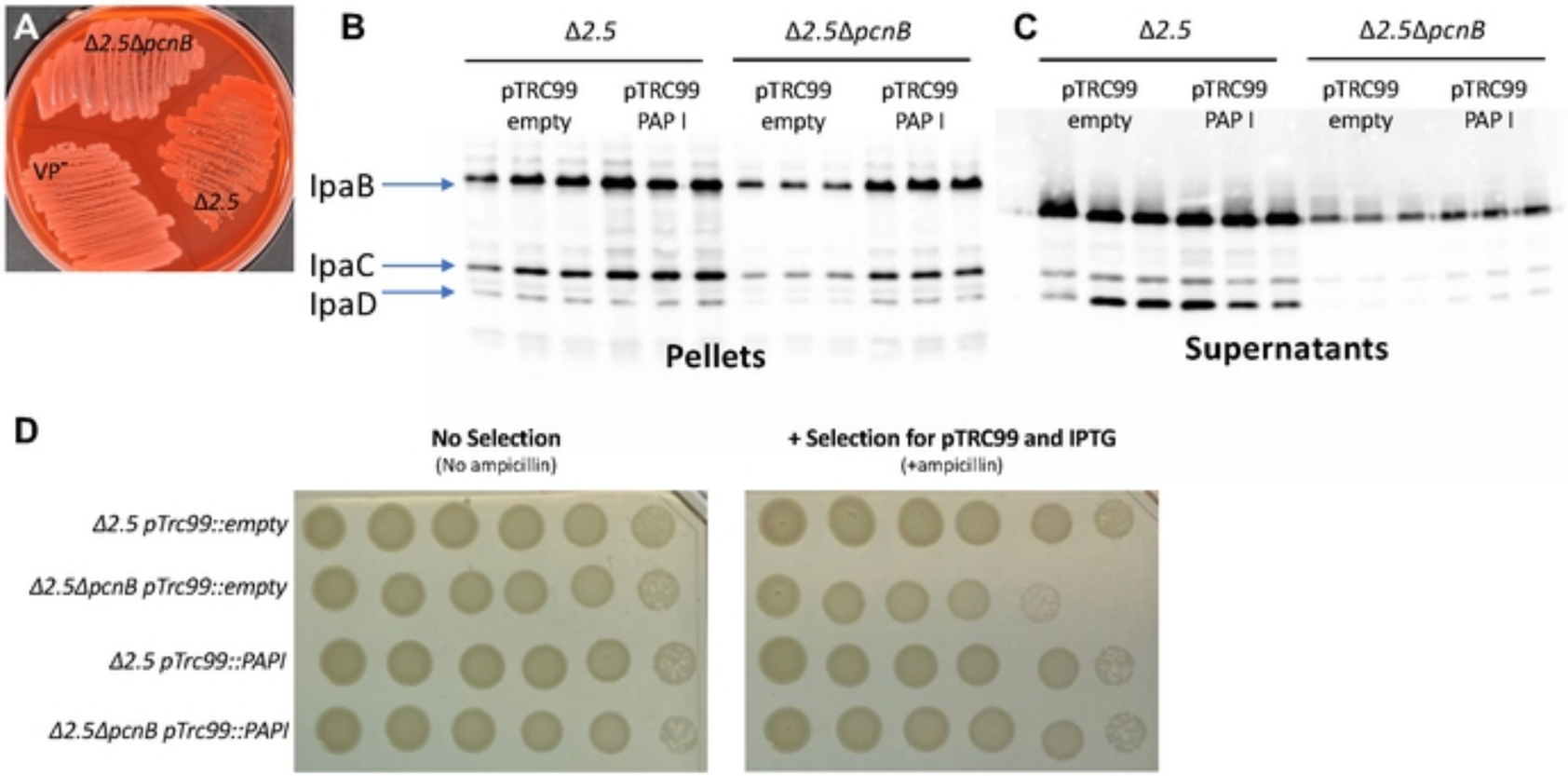
A
Δ2.5ΔpcnB
VP⁻
Δ2.5
B
Δ2.5
Δ2.5ΔpcnB
pTRC99 empty
pTRC99 PAP I
pTRC99 empty
pTRC99 PAP I
IpaB
IpaC
IpaD
Pellets
C
Δ2.5
Δ2.5ΔpcnB
pTRC99 empty
pTRC99 PAP I
pTRC99 empty
pTRC99 PAP I
Supernatants
D
No Selection
(No ampicillin)
+ Selection for pTRC99 and IPTG
(+ampicillin)
Δ2.5 pTrc99::empty
Δ2.5ΔpcnB pTrc99::empty
Δ2.5 pTrc99::PAPI
Δ2.5ΔpcnB pTrc99::PAPI